Keran Ma, Lynsie A. M. Thomason and JoAnne McLaurin

Department of Laboratory Medicine and Pathobiology, University of Toronto, Toronto, Ontario, Canada

scyllo-Inositol, Preclinical, and Clinical Data for Alzheimer's Disease

Abstract

Preclinical development of *scyllo*-inositol for the treatment of Alzheimer's disease (AD) has been investigated in both *in vitro* and *in vivo* models with positive results. *scyllo*-Inositol stabilized a small conformer of Aβ42 *in vitro*, neutralized cell derived Aβ trimers and promoted low molecular weight Aβ species *in vivo*. These interactions resulted in decreased neuronal toxicity, increased long-term potentiation (LTP) and ablation of cognitive deficits in multiple mouse models of AD. *scyllo*-Inositol bioavailability, pharmacokinetics, and small animal toxicology studies demonstrated the potential for translation to human patients. The results of Phase I and Phase II clinical trials for AD are presented. Furthermore, the use of this compound for imaging and other amyloid related disorders is discussed.

I. Introduction

scyllo-Inositol has been referred to by a number of names over the course of preclinical and clinical development. Specifically, *scyllo*-inositol has been called *scyllo*-cyclohexanehexol, 1,3,5/2,4,6-cyclohexanehexol, AZD-103, and ELND005, all of which refer to the same compound. The discovery and developmental timeline of *scyllo*-inositol is illustrated in Fig. 1. The use of *scyllo*-inositol as a potential Alzheimer's disease (AD) therapeutic began with the investigations into the mechanism of Aβ-fibril formation, the mechanism of Aβ-mediated toxicity, and the role of Aβ-lipid interactions in these processes (Fenili et al., 2010). Early on it was discovered

Advances in Pharmacology, Volume 64
1054-3589/12 $00.00

http://dx.doi.org/10.1016/B978-0-12-394816-8.00006-4

that incubation of Aβ40 and Aβ42 with acidic phospholipids resulted in a random to β-structural transition of Aβ peptides and subsequent disruption of lipid bilayers (McLaurin & Chakrabartty, 1996). Of the acidic phospholipids tested, phosphatidylinositol efficiently induced a β-structure in Aβ42 (McLaurin & Chakrabartty, 1997). To elucidate the component of phosphatidylinositol responsible for β-structural induction, the headgroup,

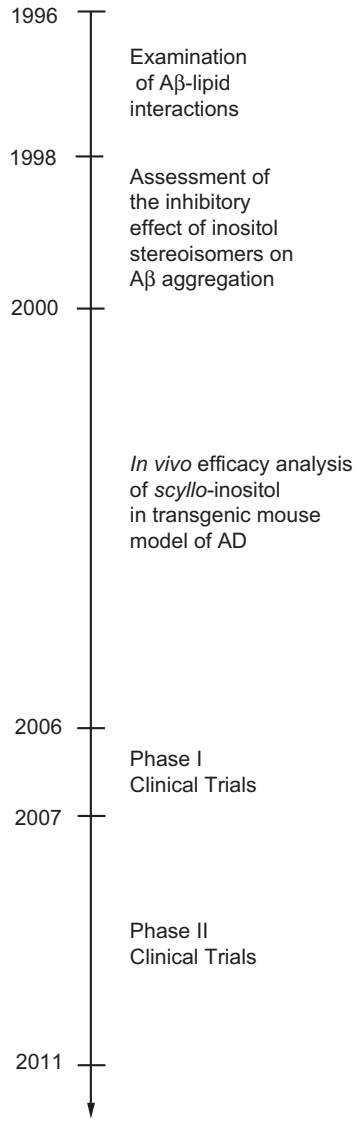

FIGURE 1 Timeline of the discovery and development of *scyllo*-inositol.

fatty acyl chains, and phosphorylation status were examined. It was found that the headgroup of phosphatidylinositol, *myo*-inositol, induced an immediate β-structure transition of Aβ42, but not when phosphorylated (McLaurin et al., 1998). An important finding of this study was that while *myo*-inositol induced a β-structure in Aβ42, it did not lead to the formation of fibrils as was seen when Aβ was incubated alone or with phosphatidylinositol (McLaurin et al., 1998); thus, the beginning of a 14-year journey that still continues.

II. Preclinical Development of *scyllo*-Inositol

The *myo*-inositol-induced formation of stable Aβ42 micelles probed the investigation of other inositol stereoisomers (McLaurin et al., 2000). Inositols are polyols consisting of a six carbon ring structure with a hydroxyl group at each carbon position, also known as cyclohexane-1,2,3,4,5,6-hexol with a chemical formula of $C_6H_{12}O_6$ (Bouveault, 1894; Posternak, 1965). There are nine stereoisomers of inositol based on the orientation of the hydroxyl groups. *myo*-Inositol is the most abundant stereoisomer. Other stereoisomers include *scyllo*-inositol, *cis*-inositol, *epi*-inositol, *allo*-inositol, *muco*-inositol, *neo*-inositol, and the enantiomers *D-chiro*- and *L-chiro*-inositols.

epi-Inositol, *scyllo*-inositol, and *chiro*-inositol were all tested for an effect on Aβ structural transition and prevention of fibril formation (Fenili et al., 2010; McLaurin et al., 2000). Both *epi*-inositol and *scyllo*-inositol, similar to *myo*-inositol, induced a β-structure transition in Aβ42 that did not lead to fibril formation (McLaurin et al., 2000). *chiro*-Inositol on the other hand did not induce a β-structure in Aβ42 and when incubated with Aβ42 lead to the formation of fibrils that were indistinguishable from those formed when Aβ42 was incubated alone (McLaurin et al., 2000). The inositol stereoisomers differ in the orientation of their hydroxyl groups and thus each has a different pattern of hydrogen donors and acceptors (McLaurin et al., 2000). These slight differences in the molecules lead the McLaurin group (2000) to hypothesize that the pattern of hydrogen donors and acceptors may play an important role in determining the structure–activity relationship with Aβ. A more in depth discussion of the structure–function relationship of the inositols is covered later in the chapter.

More recently, two groups confirmed the inhibition of Aβ aggregation by *scyllo*-inositol using very different *in vitro* assays (Park et al., 2011; Zhao et al., 2011). Zhao and colleagues developed novel ELISA assays for screening Aβ aggregation inhibitor compounds based on the fact that Aβ oligomers adopt a conformation that has an exposed N-terminus and buried C-terminus thus providing a measure of differential signal for compounds that affect early stages of oligomer formation (Zhao et al., 2011).

In these assay systems, *scyllo*-inositol was shown to inhibit Aβ42 oligomerization as well as shift the Aβ42 oligomerization equilibrium toward a monomeric state. These results were confirmed using dynamic light scattering. In contrast, Park and colleagues developed a yeast-based screen to identify inhibitors of Aβ42 specific oligomerization (Park et al., 2011). In this yeast model, Aβ42 was fused to the essential functional domain of the translation release factor, Sup35 (MRF), which was overexpressed; this resulted in the formation of SDS-stable low *n*-oligomers. In this system, *scyllo*-inositol decreased oligomer formation by greater than 50% and rescued the growth defect without an increase in cell death. These results are consistent with the previous *in vitro* studies that demonstrated *scyllo*-inositol induced inhibition of Aβ oligomerization (McLaurin et al., 2000; Townsend et al., 2006).

Since the accumulation of Aβ oligomers/fibrils is believed to be a key component in AD pathology (Karran et al., 2011), the effect of compounds on the inhibition of fibrillogenesis is of great interest. In order for any compound to undergo further investigation as a potential therapeutic, the toxicity of the complex formed in the presence of Aβ must be tested (Shaw et al., 2011). It is well documented that Aβ oligomers are toxic, therefore compounds that favor the stabilization of oligomers may enhance toxicity as was seen for the naphthalene sulfonates and some *N*-methylated peptides (Ferrao-Gonzales et al., 2005; Kokkoni et al., 2006); however, off-fiber pathway oligomers are not toxic as was shown with resveratrol and RS-0406 compounds (Feng et al., 2009; Walsh et al., 2002). The differentiation of these two oligomers by structure alone is not always possible and hence the added information given by the toxicity assay is necessary for clinical development (Shaw et al., 2011). Preincubation of Aβ42 with *myo*-inositol, *epi*-inositol, or *scyllo*-inositol led to the increased survival of nerve growth factor (NGF)-differentiated PC-12 cells and primary neuronal cultures compared to neurons exposed to Aβ42 alone (McLaurin et al., 2000). Further, when Aβ42 was incubated with PC-12 cells, it accumulated on the surface of the cells. However, *myo*-, *epi*-, and *scyllo*-inositol inhibited the accumulation of Aβ42 on the cell surface (McLaurin et al., 2000). This led to the proposal that the observed reduction of toxicity may be in part a result of the decreased interaction of Aβ with the cell membrane (McLaurin et al., 2000). These combined results demonstrated that three of the nine inositol stereoisomers demonstrated *in vitro* properties that are conducive to further investigation.

Since *myo*-, *epi*-, and *scyllo*-inositol were all successful at inhibiting fibrillogenesis *in vitro*, their efficacy *in vivo* was assessed. These three inositol stereoisomers were administered to a transgenic mouse model of AD—the TgCRND8 model (Fenili et al., 2010; McLaurin et al., 2006). The TgCRND8 mouse model is considered an aggressive model due to the overexpression of the human amyloid precursor protein (APP695) that contains

the "Swedish" mutation (K670N, M671L) and the "Indiana" mutation (V717F) (Chishti et al., 2001). These mice express a high Aβ42:40 ratio that results in the development of amyloid deposits and cognitive deficits by 3 months of age (Chishti et al., 2001). Further, these mice have accelerated mortality, a common consequence of AD in human patients (Chishti et al., 2001; McLaurin et al., 2006). Treatment of TgCRND8 mice with *myo*-inositol was not effective since no significant cognitive benefit was observed, which may not be surprising because *myo*-inositol levels are highly regulated within the central nervous system (CNS) (McLaurin et al., 2006; Fenili et al., 2007). Treatment with *epi*-inositol appeared to have effects at the early stages of disease, 4 months of age; however, as the disease progressed no beneficial effects were detected (McLaurin et al., 2006). In contrast to *myo*- and *epi*-inositol, *scyllo*-inositol treatment improved AD-like pathology when given prophylactically starting at 6 weeks of age and continuing until 4 and 6 months of age (McLaurin et al., 2006). Treatment of TgCRND8 mice with *scyllo*-inositol increased survival from 42% to 72% at 6 months of age ($p = 0.02$) and the treated mice showed a complete improvement of cognitive deficits when assessed by the Morris water maze test of spatial memory at both ages (McLaurin et al., 2006).

Further confirmation of improved cognition in the treated TgCRND8 mice was the reduction of synaptic toxicity illustrated by 146% increase in synaptophysin positive boutons and cell bodies in the hippocampus at 6 months of age (Fenili et al., 2010; McLaurin et al., 2006). *scyllo*-Inositol treatment reduced total Aβ40 ($p < 0.001$) and Aβ42 ($p < 0.05$) and decreased parenchymal plaque load throughout the brain ($p < 0.05$) (McLaurin et al., 2006). Fig. 2 shows Aβ plaques, in brown, at 6 months of age in TgCRND8 untreated (A and B) and *scyllo*-inositol treated (D and E) mice in the hippocampus and cortex, respectively. High magnification images of untreated (2C) and *scyllo*-inositol treated (2F) TgCRND8 brain illustrate the decrease in mean plaque size as a result of *scyllo*-inositol treatment. Treatment also decreased the size of cerebrovascular Aβ deposits and reduced the percentage of brain area covered by vascular amyloid. Treatment with *scyllo*-inositol reduced the amount of high molecular weight Aβ species and increased the levels of trimeric and monomeric Aβ species, suggesting that the beneficial effects of *scyllo*-inositol are due to the inhibition and/or disaggregation of high molecular weight Aβ species (McLaurin et al., 2006). Lastly, *scyllo*-inositol improved the neuroinflammatory status of treated TgCRND8 mice through the reduction of microgliosis and astrogliosis (McLaurin et al., 2006). Decreased astrogliosis is shown in Fig. 2 where *scyllo*-inositol treatment decreased the number of reactive astrocytes (labeled in red) throughout the hippocampus (2A) and cortex (2B) compared to that of the controls (2D, 2E). As shown in high magnification, astrogliosis is reduced surrounding Aβ plaques as well as nonplaque associated regions (2C, 2F).

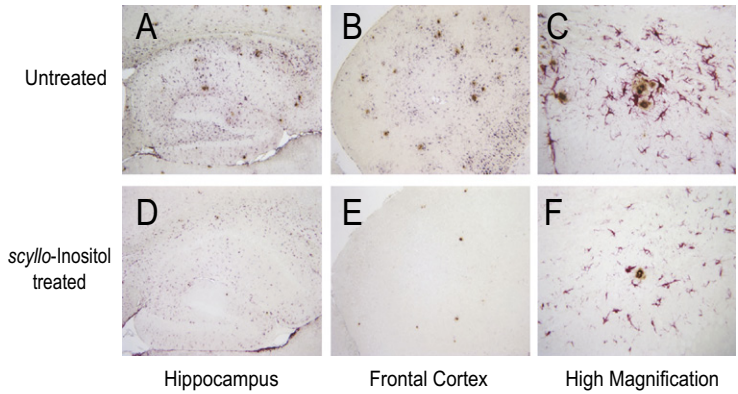

FIGURE 2 ***scyllo*-Inositol treatment decreased Aβ plaque load and reduced astrogliosis in the TgCRND8 brain at 6 months of age.** Aβ plaques are brown and reactive astrocytes are red. Aβ plaques and astrocytes in the hippocampus and cortex of untreated TgCRND8 brain are shown in A and B respectively. Decreased Aβ plaque load and astrogliosis as a result of *scyllo*-inositol treatment in the hippocampus and cortex are shown in D and E. C and F show the differences between control and *scyllo*-inositol treatment in high magnification. (Modified from McLaurin et al., 2006). For interpretation of the references to color in this figure legend, the reader is referred to the online version of this book.

It is evident that *scyllo*-inositol can inhibit the development of AD-like pathology in TgCRND8 mice when administered prior to the expression of the AD-like phenotype. However, for *scyllo*-inositol to be a treatment for AD, it would need to be effective once the disease has already begun, since AD is initiated approximately 10 years prior to the onset of clinical symptoms (Shim & Morris, 2011). To determine therapeutic potential, *scyllo*-inositol was administered to TgCRND8 mice for 28 days starting at 5 months of age (Fenili et al., 2010; McLaurin et al., 2006). At this age, the mice have significant Aβ and plaque loads as well as cognitive deficits (Chishti et al., 2001). Assessment of these mice at 6 months of age, using the Morris water maze test, showed that treated TgCRND8 mice had significantly improved performance compared to untreated TgCRND8 mice ($p = 0.01$), and their performance was not significantly different from non-transgenic littermates ($p = 0.11$) (McLaurin et al., 2006). Similar to the results of the prophylactic experiments, *scyllo*-inositol treatment after disease onset reduced insoluble Aβ40 ($p < 0.05$) and Aβ42 ($p < 0.05$) levels in the brain and significantly reduced plaque burden ($p < 0.05$) (McLaurin et al., 2006). Overall the beneficial effects were similar to those from the prophylactic studies (McLaurin et al., 2006).

Following the publication of the effects of *scyllo*-inositol on the AD-like phenotype in TgCRND8 mice, further investigation utilizing different *in vitro* and *in vivo* models confirmed the effects of *scyllo*-inositol. Townsend and colleagues found that *scyllo*-inositol could prevent Aβ-oligomer-induced inhibition of long-term potentiation (LTP) in hippocampal mouse brain

slices (Townsend et al., 2006). When *scyllo*-inositol was preincubated with Aβ or applied to cells producing Aβ, inhibition of LTP normally caused by Aβ was significantly reduced (Townsend et al., 2006). However, when *scyllo*-inositol was applied to the brain section after Aβ was applied, there was no protection of LTP (Townsend et al., 2006). The authors confirmed that protection of LTP by *scyllo*-inositol was a result of neutralization of secreted Aβ trimers (Townsend et al., 2006). Further support for *scyllo*-inositol-induced neutralization of Aβ oligomers comes from the observation that simultaneous application of *scyllo*-inositol and Aβ oligomers prevented oligomer-induced decrease in dendritic spine density (Shankar et al., 2007). These *in vitro* studies correlate well with the rescue of cognitive deficits in the TgCRND8 mouse studies.

The effect of *scyllo*-inositol to reverse or diminish Aβ-induced cognitive deficits in an acute model of Aβ-toxicity was examined using *in vivo* studies in rats (Townsend et al., 2006). Intracerebroventricular (ICV) injection of Aβ in rats increases switching and perseveration errors in the alternating lever cyclic ratio assay, which is a test of complex reference memory (Townsend et al., 2006). When *scyllo*-inositol is incubated with Aβ prior to ICV injection both types of errors are decreased. These errors also returned to baseline when *scyllo*-inositol was orally administered for 3 days prior to ICV injection of Aβ (Townsend et al., 2006). These findings suggest that *scyllo*-inositol is effective in an acute AD model.

It is evident from imaging studies that the amyloid load and presumably the Aβ load in patients varies greatly (Devanand et al., 2010). Since we are presently unable to predict the Aβ load in patients with AD, understanding the effectiveness of a potential compound in various mouse models of different genetic backgrounds and varying Aβ loads is important for translation to a highly variable AD population. In order to determine the effect of *scyllo*-inositol in a more aggressive transgenic model of AD, the treatment of disease-bearing PS1 (M146L + L286V) × TgCRND8 mouse (PS1 × APP) (Chishti et al., 2001) with *scyllo*-inositol for 4 weeks was examined (DaSilva et al., 2009; McLaurin, unpublished results). The PS1 × APP mouse model exhibits high Aβ load and significant plaque burden by 1 month of age, and continues to rapidly accumulate Aβ to that of end-stage AD patients by 2 months of age; this is in comparison to TgCRND8 singly-transgenic mice which have Aβ load equivalent to end-stage AD patients at 7 months of age (Chishti et al., 2001). The high expression of Aβ is the result of incorporation of two familial AD mutations into both APP and presenilin-1. The rapid accumulation of Aβ plaques is the result of the high Aβ42:Aβ40 ratio, 14:1, and the greater propensity of Aβ42 to aggregate. Since Aβ is produced at supra-physiological levels, any significant changes in amyloid load seen in this model would be indicative of a potent compound.

Effective inhibition of Aβ plaque deposition once treatment was initiated demonstrated that even at supra-pathological Aβ levels, *scyllo*-inositol

was highly potent (DaSilva et al., 2009). Both plaque count and percentage brain area occupied by plaques were reduced by 50% (Fig. 3A and B), which is greater than the reductions seen in TgCRND8 mice treated at 5 months of age for 28 days (McLaurin et al., 2006). Insoluble Aβ40 and Aβ42 and soluble Aβ42 were also significantly reduced after *scyllo*-inositol treatment with reductions that were equivalent to those observed in TgCRND8 mice (McLaurin et al., 2006). Previous studies demonstrated that *scyllo*-inositol decreased high molecular weight Aβ oligomers and populated trimeric and monomeric Aβ species thereby rescuing cognitive deficits in this model (McLaurin et al., 2006). Here soluble oligomeric species (greater than 40kDa) increased following treatment, while monomeric, dimeric, and trimeric Aβ aggregates were also increased (Fig. 3C). The high level of Aβ expression in this mouse model may preclude effective removal of soluble Aβ species. Moreover, these results correlate with previous vaccine studies in TgAPP mice, which demonstrate a robust decrease in Aβ plaques and cognitive improvements with no change in total brain Aβ levels (Janus et al., 2000).

Recent reports have pointed to soluble Aβ oligomers as the neurotoxic species capable of inhibiting LTP, learning, and memory (Klyubin et al., 2005; Townsend et al., 2006; Walsh et al., 2002). Ultrastructurally soluble Aβ oligomers have been localized to cell processes in AD brains (Kokubo et al., 2005), and appear to be targeted to synapses in cultured hippocampal neurons (Lacor et al., 2004). Exposure of neurons to oligomers causes abnormal spine morphology, decreased spine density, and decreased expression of synaptic markers such as synaptophysin (Ishibashi et al., 2006; Lacor et al., 2007; Shankar et al., 2007). Indeed, decreases in synaptophysin, syntaxin, and dynamin-1 have been correlated with cognitive decline in transgenic models of AD (Kelly et al., 2005; Oakley et al., 2006). Treatment with *scyllo*-inositol after the appearance of Aβ oligomers (at 1 month) appears to restore synaptic architecture, as seen by increases in the expression of the presynaptic markers synaptophysin, syntaxin, synapsin, and dynamin-1 (Fig. 3D; DaSilva et al., 2009; McLaurin unpublished results). This was seen irrespective of the increased levels of monomers, dimers, trimers, and higher molecular-weight oligomers (>40kDa). This is in agreement with previous findings where treatment with *scyllo*-inositol increased synaptophysin levels in both prophylactic and treatment paradigms (McLaurin et al., 2006). Thus, *scyllo*-inositol protected against synaptic dysfunction in PS1 × APP mice and demonstrated the potency of *scyllo*-inositol in an aggressive model of AD.

Another mouse model, 5 × FAD, which contains five familial AD mutations—APP 695 K670N/M679L (Swedish), I716V (Florida), V717I (London), and PS1 M146L and L286V mutations, was utilized as an alternate model of Aβ pathology (Oakley et al., 2006). These mice show cerebral amyloid plaques and gliosis by 2 months of age and have increased Aβ42

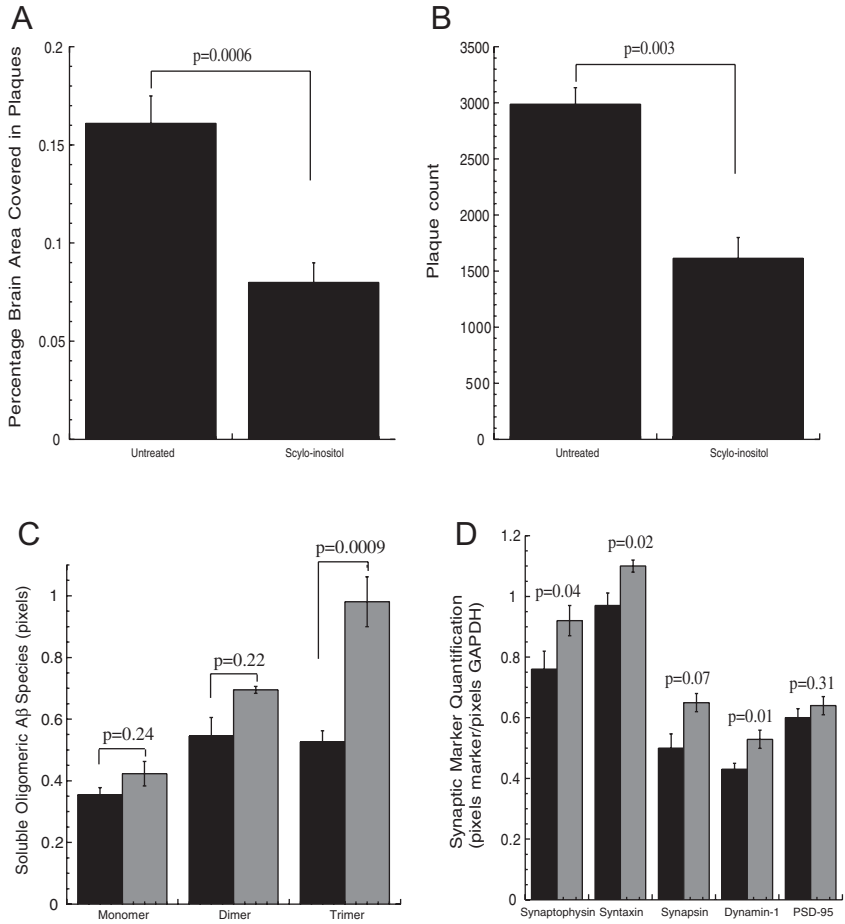

FIGURE 3 **Evaluation of the effect of *scyllo*-inositol on plaque load and synaptic health in an aggressive transgenic mouse model of AD.** *scyllo*-Inositol treatment for 4 weeks starting at 4 weeks of age in PS1 × APP transgenic mouse model of AD decreased percentage brain area covered by plaques (A) and plaque count (B) by approximately 50%. *scyllo*-Inositol also increased monomeric, dimeric and trimeric Aβ (D) as well as rescued synaptic architecture as shown by the increase in synaptic markers synaptophysin, syntaxin, synapsin and dynamin-1 (E).

levels detected as early as 1.5 months of age. The 5 × FAD mice first develop plaques in the cortex and subiculum, which then progress to the hippocampus, thalamus, brain stem, and olfactory bulbs. Further, these mice display neuronal loss and exhibit memory deficits between 4 and 5 months of age (Oakley et al., 2006). Aytan and colleagues administered *scyllo*-inositol to 5 × FAD mice for 1 month after amyloid pathology was evident (Aytan et al., 2011). The *scyllo*-inositol treated mice were compared to untreated 5 × FAD wild-type mice and 5 × FAD treated mice in combination with

scyllo-inositol and R-flurbiprofen. Image analyses demonstrated that *scyllo*-inositol treated mice had 38% and 34% reduction in Aβ42 and Aβ40 containing deposits as well as parallel peptide reductions as measured by ELISA. These reductions were accompanied by improvement in performance in the radial arm water maze task of spatial memory. Surprisingly, treatment with *scyllo*-inositol in the presence of R-flurbiprofen was less effective both cognitively and pathologically than *scyllo*-inositol treatment alone (Aytan et al., 2011). These results further demonstrate the effectiveness of *scyllo*-inositol in mouse models containing varying familial mutations, genetic backgrounds, and Aβ burdens.

III. Sources of *scyllo*-Inositol

Alzheimer's Disease International estimated in 2009 that there were 36 million people suffering from dementia worldwide and this number will increase to 66 million by 2030 and 115 million by 2050. In 2010 alone, worldwide cost for dementia was $604 billion (Prince et al., 2011). For a naturally occurring compound to be used as a pharmaceutical to treat AD, it needs to be available in large quantities. Furthermore, the isolation procedures or synthetic pathways necessary to achieve this requirement must also be done in a reasonable time frame and at reasonable cost.

A. Natural Sources

scyllo-Inositol was first discovered in sharks and skates in 1858 by Staedler and Frerichs; it was extracted from the kidney, liver, spleen, and gills of the shark *Scyllium canicula* and skates *Raja batis* and *Raja clavata* (Fenili et al., 2010; Staedler & Frerichs, 1858). *scyllo*-Inositol is present in all organs of the skate *Raja erinacea*, with highest levels in the liver and kidney; it is found at a much higher concentration in most organs of skates compared to *myo*-inositol, except the brain and the peripheral nerve (Sherman et al., 1978). Skates have slow growth and low reproductive rates making them a poor choice for *scyllo*-inositol isolation in bulk quantities (Mcphie & Campana 2009; Williams et al., 2011). *scyllo*-Inositol is also found in a variety of plant tissues including coconut, soursop, flowers of dogwood, and the bark of white and English oak (Goodson, 1920; Hann & Sando, 1926; Muller, 1907; Muller, 1912). Alternatively, *scyllo*-inositol has been reported in grapes, some citrus fruit, and vegetables of the Apiaceae family (Fenili et al., 2010; Sanz et al., 2004; Soria et al., 2009). It is even found in insects such as locusts, cockroaches, and blow flies (Candy, 1967). Although many higher plants express compounds in quantities that are sufficient for raw materials for scientific and commercial applications, there are exceptions such as inositol and β-carotene which are very expensive due to the

extraction, isolation, and purification process (Balandrin et al., 1985; Fenili et al., 2010).

B. Chemical Synthesis

Besides natural sources, *scyllo*-inositol can be synthesized chemically. *scyllo*-Inositol has been synthesized historically by a number of synthetic routes including from halobenzenes, tetrahydroxyquinone, sugars, and other inositols (Anderson & Wallis, 1948; Angyal et al., 1995; Kowarski & Sarel, 1973; Mandel & Hudlicky 1993; Watanabe et al., 1987; Tagliaferri et al., 1990). However, these methodologies have low efficiencies for industrial scale use. More recent methods demonstrate increased efficiencies and are discussed here. One methodology involves the didehydroxylation of *myo*-inositol via the intermediate conduritol B to produce gram scale quantities of *scyllo*-inositol. In this method, *myo*-inositol diols are converted to conduritol B, which was epoxidized, followed by ring opening to produce *chiro*- and *scyllo*-inositol isomers with the *scyllo*-inositol isomer in much lower yield (Chung & Kwon, 1999). Although this synthetic route produced gram scale quantities, the yield of *scyllo*-inositol is only 16%.

To increase yield, Podeshwa and colleagues employed the production of inositol stereoisomers from enantiomerically pure building blocks (Podeshwa et al., 2003). These building blocks were diacetoxy-dibromocyclohex-5-ene (+) or (−), which are easily made from *p*-benzoquinone. Similar to the method by Chung and Kwon, diacetoxy-dibromocyclohex-5-ene (+) is converted to a conduritol B intermediate, which undergoes epoxidation. Regioselective opening of the epoxide yields a *scyllo*-isomer, which becomes *scyllo*-inositol after hydrogenation (Podeshwa et al., 2003). This method produces *scyllo*-inositol in much higher yield, yet requires purification steps.

To improve the yield of *scyllo*-inositol, methodological development was further employed. The use of 6-deoxyhex-5-enopyranosides as the starting compound instead of *myo*-inositol (Takahashi et al., 2001), combined with Ferrier-II carbocyclization, efficiently produces chiral-substituted cyclohexanones. This reaction was catalyzed by palladium dichloride to produce β-hydroxycyclohexanones. Stereoselective reduction of β-hydroxycyclohexanones with $NaBH_4$ resulted in *scyllo*-inositol in good yield, 86% of starting material (Takahashi et al., 2001). This method has the advantage of abundant starting material at low cost and a controlled efficient production of *scyllo*-inositol.

To further improve the yield of *scyllo*-inositol, Sarmah and Shashidhar developed another synthetic scheme (Sarmah & Shashidhar, 2003). The overall yield to produce *scyllo*-inositol from *myo*-inositol via an orthoformate intermediate was 64% using this method. In this method, *myo*-inositol was

first converted to *myo*-inositol orthoformate using a convenient high-yielding methodology without the use of time consuming chromatography (Praveen & Shashidhar, 2001). *myo*-Inositol orthoformate was then benzoylated to yield 2-benzoate. Sulfonylation of 2-benzoate with subsequent Swern oxidation and reduction produced *scyllo*-ditosylate. Through a series of methanolysis, acetylation, and aminolysis, *scyllo*-inositol orthoformate was made. The final step of hydrolysis with aqueous acid converted *scyllo*-inositol orthoformate to *scyllo*-inositol (Sarmah & Shashidhar, 2003). This methodology improved upon the synthetic strategies based on *myo*-inositol, but it still had a lower yield than some of the previous synthetic pathways.

Although chemical synthesis of pure *scyllo*-inositol has improved with yields up to 86% from starting material, this represents a labor intensive process including purification steps.

C. Biological Synthesis

Biological synthesis of *scyllo*-inositol started with the discovery of enzymes that convert the abundant *myo*-inositol to the other stereoisomers (Larner et al., 1956; Ramaley et al., 1979). In 1977, Hipps and colleagues discovered an epimerase from bovine brain extract, specifically in the unbound DEAE-cellulose fraction, which converts *myo*-inositol to *neo*- and *scyllo*-inositol (Hipps et al., 1977). This epimerase functions at an optimal pH of 9.5 in the presence of dithiothreitol. Incubation of the epimerase with NADP+ allows for a much greater conversion of *myo*-inositol to *neo*- and *scyllo*-inositol than with NAD+ (Hipps et al., 1977). Although the presence of the epimerase in bovine brain has been known for a long time, utilization of this enzyme for translation into biological or industrial use has not been reported.

Evolutionary studies have shown that archaea, several bacteria, and eukaryotes synthesize and utilize *myo*-inositol for various functions (Michell, 2008). More recently it has also been recognized that *scyllo*-inositol can be utilized as readily as *myo*-inositol in these organisms (Michell, 2008). Gram positive bacteria, *bacillus subtilis*, have a unique inositol metabolism pathway that involves *myo*-, *chiro*-, and *scyllo*-inositols (Holub, 1986; Yoshida et al., 2008). This bacterial strain was genetically modified in 2006 to generate a cell factory for the production of *chiro*-inositol after the discovery that *chiro*-inositol may have a benefit for diabetes (Yoshida et al., 2006). More recently, this same system, *bacillus subtilis,* was modified as a cell factory to convert *myo*-inositol to *scyllo*-inositol as an inexpensive method to produce *scyllo*-inositol (Yamaoka et al., 2011). Under normal conditions, *bacillus subtilis* convert *myo*-Inositol to *scyllo*-inosose by the *myo*-inositol dehydrogenase, IolG, coupled with the reduction of NAD^+ to NADH. Multiple step degradation of *scyllo*-inosose produces the final *myo*-inositol degradation products—dihydroxyacetone

phosphate and acetyl-CoA. Alternatively, *scyllo*-Inosose can be converted to *scyllo*-inositol by the distinct *myo*-inositol dehydrogenase, IolW, coupled with NADPH oxidation to $NADP^+$. The identification of the *iolE41* missense mutation allele in genetically modified *Bacillis subtilis* results in interference with the degradation of *scyllo*-inosose. The resultant intracellular accumulation of *scyllo*-inosose increased the production of *scyllo*-inositol from *scyllo*-inosose by IolW (Yamaoka et al., 2011). This cell factory method of *scyllo*-inositol production converts close to 10g/L of *myo*-inositol to *scyllo*-inositol in 48h.

An alternate method for *scyllo*-inositol production involves the bioconversion of *myo*-inositol to *scyllo*-inositol using microorganisms optimized for industrial-scale production (Reddy et al., 2011). In this bioconversion, microorganisms of the *Acetobactor* and *Burkholderia* genera were used to convert *myo*-inositol to *scyllo*-inosose and *scyllo*-inositol in a fermentation mixture. This mixture is then treated with a base and subjected to heat to degrade *scyllo*-inosose and lyse the cells. The remaining bioconversion product, *scyllo*-inositol, is reacted with boric acid and sodium hydroxide to form *scyllo*-inositol-diborate-disodium salt complex. This complex is then hydrolyzed to yield crude *scyllo*-inositol before crystallization to produce the final product of *scyllo*-inositol.

Yamaguchi and colleagues identified a novel NAD^+-independent *myo*-inositol 2-dehydrogenase in *Acetobacer*, strain AB10253, which catalyzes an efficient conversion of *myo*-inositol to *scyllo*-inosose (Yamaguchi et al., 2004). AB10253 or any microorganisms containing NAD^+-independent *myo*-inositol 2-dehydrogenase can be used to produce *scyllo*-inositol from *myo*-inositol. The resulting product from the bioconversion of *myo*-inositol, *scyllo*-inosose can be reduced to *scyllo*-inositol via *scyllo*-inositol dehydrogenase in a NADH/NADPH-dependent manner. Once *scyllo*-inositol is produced in the microorganism, it is precipitated to form a complex of low solubility. This complex is then dissolved in acid and purified by either ion exchange resin or a water-soluble organic solvent extraction to produce *scyllo*-inositol.

These combined bioconversion studies show the potential for the production of pharmaceutical quantities of *scyllo*-inositol at reasonable costs. The method by Yamuguchi and colleagues was utilized for both the preclinical development and Phase I and II clinical trials of *scyllo*-inositol.

IV. Bioavailability and Metabolism

The next major hurdle normally encountered for the development of CNS drugs is brain bioavailability. In fact many active compounds fail to proceed further in development due to the lack of adequate CNS bioavailability. For an aging population and long-term delivery, oral bioavailability

is the most convenient and readily compliant method for drug administration. In the preclinical studies, oral administration of *scyllo*-inositol had beneficial effects; however, the mechanism of transport of *scyllo*-inositol across the blood–brain barrier (BBB) was unknown.

To prove that orally administered *scyllo*-inositol was acting within the CNS, gas chromatography/mass spectrometry was performed to determine *scyllo*-inositol levels in the CSF and brain after oral administration in the TgCRND8 mouse model (Fenili et al., 2007). Analysis of *scyllo*-inositol *ad libitum* treatment showed a 16-fold increase ($p < 0.001$) in CSF *scyllo*-inositol levels and a 7.6-fold increase ($p < 0.001$) in brain *scyllo*-inositol levels (Fenili et al., 2007). *scyllo*-Inositol treatment did not significantly alter *myo*-inositol levels in the CSF, which is advantageous since *myo*-inositol is an organic osmolyte and is involved in cell signaling in the brain (Fenili et al., 2007). Furthermore, *scyllo*-inositol levels were significantly higher after *ad libitum* treatment compared to a single daily dose. This would suggest that receiving multiple doses throughout the day over the course of treatment may allow for high CNS *scyllo*-inositol levels to be maintained. A twice daily gavage regiment resulted in similar cognitive and pathological readout measures as was seen for *ad libitum* administration (McLaurin et al., 2006).

scyllo-Inositol levels in the brain can also be measured using magnetic resonance spectroscopy (MRS). MRS is useful for detecting neurochemical changes in the brain of AD mouse models and has been utilized to distinguish AD from other dementias in patients (Watanabe et al., 2010). Using two mouse models of AD, *scyllo*-inositol levels were measured from brain tissue extracts and intact hippocampal and cortical tissue (Choi et al., 2010). The mouse models utilized in this study were the Tg2576xPS1[M146V] (Holcomb et al., 1998) while the second model was a triple transgenic, 3XTg, that expresses human APP [Swedish mutation], PS1 [M146V] and Tau [P301L] mutations (Oddo et al., 2003). The models differ not only in the inclusion of the Tau P301L mutation but also in the expression level of Aβ and genetic background. *scyllo*-Inositol was administered *ad libitum* for a final dose of 3.3mg/Kg/day, as was previously shown to be effective in mice (McLaurin et al., 2006). Isolation of tissue homogenates for solution MRS and intact brain regions for high resolution magic angle spinning spectroscopy analyses of treated and untreated mice were harvested (Choi et al., 2010). Analyses of tissue homogenates demonstrated a 3-fold increase in *scyllo*-inositol treated versus untreated mice, which was confirmed using magic angle spectroscopy. *scyllo*-Inositol levels were increased in both the hippocampus and the frontal cortex with higher levels found in the hippocampus in both mouse models (Choi et al., 2010). These studies confirmed the increase in *scyllo*-inositol in TgCRND8 mice.

The oral availability of *scyllo*-inositol was further tested in long-term toxicology studies in rats and dogs, which demonstrated that *scyllo*-inositol

was completely orally bioavailable (http://www.transitiontherapeutics.com/media/news.php). Further development required understanding the pharmacokinetic properties of *scyllo*-inositol in the brain (Quinn et al., 2009). In order to determine brain and CSF exposure, Spraque-Dawley rats were gavaged with *scyllo*-inositol at three doses twice daily for 5 days. The concentration of *scyllo*-inositol in plasma, CSF, and frontal cortices was determined at 1–24 h after the last dose by gas-chromatography mass spectrometry (Quinn et al., 2009). Plasma *scyllo*-inositol levels increased disproportionately to dose as did CSF and brain levels. The CSF *scyllo*-inositol concentration was half plasma levels while brain was 10-fold increased over plasma and remained constant over the course of the experiment. The CSF levels decayed in parallel with the plasma levels. The absorption of *scyllo*-inositol was rapid with time of maximum uptake within 1–3 h of dosing. Brain concentrations reached 4-, 8-, and 12-fold increased levels over endogenous *scyllo*-inositol when dosed at 5, 15, and 30mg/Kg BID (Quinn et al., 2009). The combined rodent studies show that *scyllo*-inositol is CNS bioavailable, which would suggest that *scyllo*-inositol is either actively transported or passively diffused into the brain.

In 1976, it was recognized that transport of *myo*-inositol into the CNS was through a saturable transport system in the choroid plexus (Spector, 1976). Subsequently, the three inositol transporters were reported: sodium/*myo*-inositol transporter 1 (SMIT1), sodium/*myo*-inositol transporter 2 (SMIT2), and proton/*myo*-inositol transporter (HMIT). SMIT1 was the first of the inositol transporters to be discovered (Kwon et al., 1992). The discovery of SMIT2 and HMIT, similar to SMIT1, occurred through further investigations into cellular osmoregulation and general inositol transport (Kwon et al., 1992; Coady et al., 2002; Uldry et al., 2001). More recently the role of SMIT1/2 and HMIT in *scyllo*-inositol CNS bioavailablity and how this may impact the potential therapeutic effects of *scyllo*-inositol for AD have been investigated (Fenili et al., 2011).

A. Sodium/*myo*-Inositol Transporter 1

The SMIT1 is member number three of the solute carrier family five, thus is also referred to as SLC5A3 (Berry et al., 1995). SMIT1 has greater than 93% homology across human, mouse, canine, and bovine species (McVeigh et al., 2000). SMIT1 mRNA has been found in human brain, kidney, placenta, pancreas, and lung tissue, as well as in heart and skeletal muscle (Berry et al., 1995; Fenili et al., 2010). Analysis of the rat brain revealed that the choroid plexus contained the highest levels of SMIT1 mRNA, with expression also in the pineal gland, area postrema, hippocampus, locus coeruleus, suprachiasmatic nucleus, olfactory bulb, and the purkinji and granular cell layers of the cerebellum (Inoue et al., 1996). Further,

SMIT1 expression was present in neurons and glia-like cells across the rat brain (Inoue et al., 1996). The majority of *myo*-inositol transport into the brain likely occurs through SMIT1, as SMIT1–/–- mouse pups show a 92% reduction in brain *myo*-inositol and do not survive for long after birth (Berry et al., 2003). In addition, SMIT1 +/– mice show a 15% reduction of *myo*-inositol in the cortex and a 25% reduction in the hippocampus (Shaldubina et al., 2007) suggesting that SMIT1 is also important in transport of *myo*-inositol to these areas of the brain.

SMIT1 cotransports Na^+ and *myo*-inositol in a ratio of 2:1 (Matskevitch et al., 1998), but as shown in *Xenopus* oocytes expressing SMIT1, this transporter has the ability to transport numerous other sugars with the following specificity; *myo*-inositol = *scyllo*-inositol > L-fucose > L-xylose > L-glucose = D-glucose = alpha-methyl-D-glucopyranoside > D-galactose = D-fucose = 3-O-methyl-D-glucose = 2-deoxy-D-glucose > D-xylose (Hager et al., 1995; Fenili et al., 2010). The equal affinity of SMIT1 for *myo*-inositol and *scyllo*-inositol is unique among the inositol transporters (Fenili et al., 2010). SMIT1 is expressed on the plasma membrane, and in polarized cells it allows for *myo*-inositol to be taken up on the basolateral side of the cell (Kwon et al., 1992). In porcine choroid plexus cells *myo*-inositol was transported from the basolateral to the apical side of cells, resembling transport that may occur from blood to cerebral spinal fluid (Hakvoort et al., 1998).

B. Sodium/*myo*-Inositol Transporter 2

The most recently discovered inositol transporter is SMIT2, also known as member 11 of the solute carrier family five (Lin et al., 2009). The highest expression of SMIT2 mRNA has been found in heart, skeletal muscle, kidney, liver, and placenta tissue, with weaker expression also reported in the brain of humans (Roll et al., 2002). The SMIT2 sequence is 43% similar to that of SMIT1 and similarly cotransports Na^+ and *myo*-inositol in a 2:1 ratio (Coady et al., 2002; Fenili et al., 2010). However, these proteins show some interesting differences in their transport properties. SMIT2 exhibits stereospecificity transport of sugars, transporting D-glucose and D-xylose, but not their L-enantiomers (Coady et al., 2002; Ostlund et al., 1996). This is unlike SMIT1, which shows no glucose stereospecificity (Coady et al., 2002; Ostlund et al., 1996). Further, SMIT2 shows similar affinity for *myo*-inositol and D-*chiro*-inositol (Lin et al., 2009), while SMIT1 does not appear to transport D-*chiro*-inositol (Coady et al., 2002; Ostlund et al., 1996).

Both SMIT1 and 2 are expressed on the plasma membrane; however, in polarized cells such as Madin-Darby canine kidney cells, SMIT2 is located on the apical membrane while SMIT1 is located on the basolateral membrane (Bissonnette et al., 2004; Fenili et al., 2010). In these same cells,

hyperosmotic conditions increase both SMIT1 and 2 activities. Interestingly, SMIT1 activity is increased at low hyperosmotic levels and SMIT2 activity is increased at higher hyperosmotic levels (Bissonnette et al., 2008). In addition, SMIT2 activity appears to be induced quicker and peaks faster than SMIT1 (Bissonnette et al., 2008). These findings suggest that SMIT1 and SMIT2 may work together to regulate inositol levels and osmolarity within tissues.

C. Proton/*myo*-Inositol Transporter

The HMIT is one of the 13 members of the facilitative glucose transporter family of proteins (Fenili et al., 2010; Uldry et al., 2001; Zhao & Keating, 2007). Despite belonging to a family of glucose transporters, HMIT does not transport glucose or any of the related hexoses (Uldry et al., 2001). HMIT is a proton/*myo*-inositol symporter; however, rat HMITs have been shown to also transport *scyllo*-inositol, *muco*-inositol, and *chiro*-inositol, but to a lesser extent than *myo*-inositol (Uldry et al., 2001). The 90% homology of rat and human HMIT would suggest similar transport properties between these species (Fenili et al., 2010).

HMIT is expressed in small amounts in adipose tissue and the kidney, but its expression is greatest in the brain (Uldry et al., 2001). The highest expression of HMIT has been found in the cerebral cortex, hippocampus, hypothalamus, cerebellum, and brainstem (Uldry et al., 2001). HMIT expression in the brain has been localized to neurons (Di Daniel et al., 2009; Uldry et al., 2001) and astrocytes (Uldry et al., 2001). Uldry and colleagues (2004) also found that expression of HMIT on the plasma membrane was triggered by cell depolarization, protein kinase C activation, and increased intracellular calcium concentration. Conversely, Di Daniel and colleagues found that the majority of HMIT in rat and human brain is located intracellularly, and in primary rat cortical cultures was colocalized with a golgi apparatus marker (Di Daniel et al., 2009). These results suggest that HMIT plays a role in regulating intracellular inositol and may not be involved in inositol transport into cells (Di Daniel et al., 2009).

D. *myo*-Inositol Transporters as a Function of Disease

For *scyllo*-inositol to have an effect on the AD brain, transport of *scyllo*-inositol into the CNS and within the brain is required. Evidence suggests that SMIT1 and SMIT2 are likely responsible for transport of *scyllo*-inositol into the brain, and expression has been found in the three regions of the brain affected by AD, the cortex, hippocampus, and cerebellum (Fenili et al., 2011). In the TgCRND8 AD model, SMIT1 levels in these three areas were similar when the mice were 2 months of age; however, SMIT1 in the

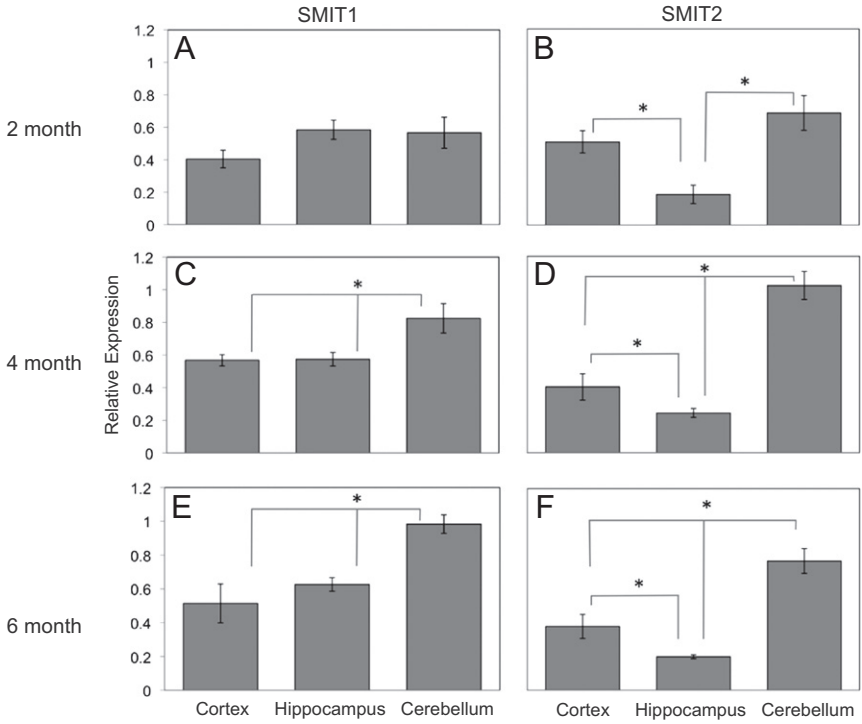

FIGURE 4 SMIT1 and SMIT2 expressions in the TgCRND8 brain as Aβ pathology advances. SMIT1 and SMIT2 expressions in the cortex, hippocampus and cerebellum in the TgCRND8 brain are not altered by age or disease progression.* $p < 0.05$.
(Reproduced from Fenili et al., 2011)

cerebellum were significantly higher than in the cortex and hippocampus at 4 and 6 months of age ($p < 0.05$). In contrast, in 2, 4, and 6 month old TgCRND8 mice, SMIT2 levels in the cortex and cerebellum were significantly higher than hippocampal levels ($p < 0.05$) (Fenili et al., 2011). These data suggest that SMIT1 and SMIT2 expression in the brain remained stable with both age and advancing Aβ pathology (Fig. 4; Fenili et al., 2011). Further it would suggest that the areas of the brain most affected by AD may have adequate *scyllo*-inositol availability even in the advanced stages of the disease.

E. Efflux

It is at least somewhat clear how *scyllo*-inositol gains entry into the brain and into cells. However, to date, there have been no studies focused specifically on *scyllo*-inositol efflux from cells. This is likely due to the fact that the function of endogenous *scyllo*-inositol has not been elucidated.

Work has been done on the efflux of the more abundant of the inositol stereoisomer, *myo*-inositol (Seaquist & Gruetter, 1998). Experiments using NT2-N neurons, primary rat astrocyte cultures, and neuroblastoma cells all suggest that *myo*-inositol efflux occurs through a volume-sensitive organic osmolyte-anion channel (VSOAC) (Isaacks et al., 1999; Loveday et al., 2003; Novak et al., 2000). *myo*-Inositol efflux is stimulated by hypo osmotic conditions and to some extent can be regulated by protein kinase C activity and intracellular Ca^{2+} levels (Loveday et al., 2003; Novak et al., 2000). While VSOAC is a nonselective Cl^- channel, it is hard to predict whether it may be involved in *scyllo*-inositol efflux.

Similar to efflux, very little is known about the degradation pathway of *scyllo*-inositol. At least some of the *scyllo*-inositol in the body is removed by direct excretion in the kidney, as *scyllo*-inositol has been identified in human urine (Yap et al., 2010; reviewed in Sherman et al., 1968). It is also possible that *scyllo*-inositol is converted into *myo*-inositol, which is then degraded through pathways in the kidney and liver. In bovine brain extracts, an $NADP^+$-dependent epimerase was identified that was capable of converting *myo*-inositol to *scyllo*-inositol and *neo*-inositol (Hipps et al., 1977). Further, in rats and rabbits it was found that *scyllo*-inositol and *myo*-inositol were able to interconvert through the intermediate *myo*-inosose-2 (Sherman et al., 1968). It should also be noted that *scyllo*-inositol levels in the CNS have been linked to *myo*-inositol levels; thus it has been speculated that *scyllo*-inositol functions as a precursor for *myo*-inositol or may be a byproduct of its metabolism (Fisher et al., 2002). Although speculative, another possibility is that *scyllo*-inositol may be degraded in the same pathway as *myo*-inositol, but without conversion to *myo*-inositol.

V. Human Clinical Trials of *scyllo*-Inositol as an AD Therapeutic

With successful results from preclinical studies, *scyllo*-inositol was approved for Phase I human clinical trial in Canada. This Phase I trial was single blinded, randomized, and placebo controlled with 12 healthy volunteers (http://www.transitiontherapeutics.com/media/news.php). Escalating doses of *scyllo*-inositol were administered to these subjects and favorable profiles of pharmacokinetics, safety, and tolerability were demonstrated. The United States Food and Drug Administration then approved a Phase I clinical trial in the United States. Overall, approximately 110 subjects participated in the Phase I clinical study and *scyllo*-inositol showed favorable safety profile and tolerability (http://www.transitiontherapeutics.com/media/news.php; Fenili et al., 2010). The pharmacokinetics of *scyllo*-inositol was assessed in the brain, CSF, and plasma in healthy volunteers. *In vivo* *scyllo*-inositol levels can be measured noninvasively using MRS (Garzone

et al., 2009). Healthy men between the ages of 24–53 were given 2000mg doses of *scyllo*-inositol BID for 10 days. MRS was used to quantify the brain concentration of *scyllo*-inositol in the gray and white matter, the posterior cingulate gyrus, and left parietal lobe, respectively. *scyllo*-Inositol levels were determined with creatine as the reference and found to increase from baseline to day 8 in all brain regions. In this study, plasma *scyllo*-inositol levels reached steady state in 5–6 days and CSF levels increased throughout the 10 days of the experiment (Garzone et al., 2009). These studies in combination demonstrated that *scyllo*-inositol is available orally and crosses the BBB to reach levels that are effective in animal models of AD.

Following safety and pharmacokinetic analyses of *scyllo*-inositol in Phase I clinical trial, *scyllo*-inositol underwent a double-blind, randomized, dose-ranging, and placebo-controlled Phase II clinical trial (Salloway et al., 2011; Fenili et al., 2010). Based on the pharmacokinetic and Phase I studies, three doses of 250, 1000, and 2000mg BID of *scyllo*-inositol were chosen. Subjects recruited for the clinical trial were between the ages of 50–85 with probable AD as determined by the National Institute of Neurological and Communicative Disorders and Stroke and the Alzheimer's Disease and Related Disorders Association, with a Mini-Mental State Examination score between 16–26, Rosen Modified Hachinski score≤4, and a magnetic resonance imaging (MRI) scan indicating AD but healthy otherwise. The mild or moderate AD patients were randomly assigned to either the placebo group or one of the three groups of increasing *scyllo*-inositol doses, with each group consisting of 84–91 subjects. The efficacy of *scyllo*-inositol was measured by a battery of cognitive tests expressed as changes from baseline to week 78 of treatment. The Neuropsychological Test Battery (NTB) and the Alzheimer's Disease Cooperative Study-Activities of Daily Living (ADCS-ADL) were chosen as primary tests and outcome measures from the Alzheimer's Disease Assessment Scale Cognitive Subscale (ADAS-Cog), Clinical Dementia Rating-Sum of Boxes (CDR-SB), and the Neuropsychiatric Inventory (NPI) were assessed as secondary outcome measures (Salloway et al., 2011). In addition, brain ventricular volume, whole brain volume, hippocampal volume, and cortical ribbon thickness at 78 weeks of treatment were assessed using MRI. Two subsets of patients were also assessed for *scyllo*-inositol and *myo*-inositol levels in the brain using MRS and CSF. Levels of Aβ and tau were analyzed in CSF samples as biomarkers of disease progression.

One predesignated subset analysis was to determine the population pharmacokinetic properties of *scyllo*-inositol in AD patients (Liang et al., 2009). Data analyses demonstrated that plasma concentrations of *scyllo*-inositol reached steady state no later than 12 weeks of administration and concentrations were proportional to the dose. The CSF/brain concentrations reached steady state at 24 weeks and reached saturation above 1000mg BID. Overall, the patient pharmacokinetics showed moderate absorption, rapid distribution from vascular to brain with a rate-limiting step associated with a slow

clearance (Liang et al., 2009). The clearance of *scyllo*-inositol was slower in AD patients versus healthy controls, in males versus females, and as a function of renal activity (Liang et al., 2009). These data provide a pharmacokinetic model that was utilized in the analyses of exposure–response in the Phase II trial.

To determine the overall safety of *scyllo*-inositol treatment in AD patients, monitoring included assessment of treatment emergent adverse effects (TEAE), clinical laboratory tests, electrocardiograms, vital signs data, and MRI every 6 months (Salloway et al., 2011). The overall incidence of TEAE was not significantly different between the groups or as a function of ApoE ε4 genotype. However, the incidence of withdrawals was greater in the two higher doses and the number of serious adverse effects was greater in the treatment groups versus the placebo. The incidence of serious infections as well as neurologic and psychiatric adverse effects was lower in the mild AD patient population. The overall incidence of serious adverse effects was similar between mild and moderate patients. The independent safety monitoring committee analyzed the data at 48 weeks and reported more infections in the 2000mg dose and a higher incidence of death in the two highest doses (http://ir.elan.com/phoenix.zhtml?c=88326&p=irol-newsArticle&ID=1365793&highlight=; Salloway et al., 2011). Although 9 of the 10 deaths were not directly attributed to *scyllo*-inositol, those doses were electively removed from the trial. The lower dose was continued and no further deaths were reported. The only clinical laboratory measure that was reported to change was a dose-dependent decrease in uric acid. The mechanism of *scyllo*-inositol-induced infections and lower uric acid levels are unknown; however, they are under investigation (Salloway et al., 2011).

The discontinuation of the two highest doses resulted in the cognitive endpoint analyses being based on 82 placebo and 84 patients treated with 250mg *scyllo*-inositol BID (Salloway et al., 2011). Overall, none of the primary or secondary endpoints reached statistical significance. The clinical trial design included subgroup analyses of mild AD, moderate AD, ApoE ε4 carriers, and noncarriers. There were no statistically significant changes for any cognitive endpoint for the moderate AD group or effect of ApoEε4 genotype. Subgroup analysis on *scyllo*-inositol efficacy in compliant mild AD patients showed that the 250mg dose of *scyllo*-inositol treatment was significantly different compared to placebo controls as measured by the NTB *z*-score ($p = 0.007$) (Salloway et al., 2011). Although overall, including both mild and moderate patients, NTB did not show a significant difference in the 250mg treated patients compared to placebo. The effect in mild population may be the result of the NTB having greater sensitivity in evaluating mild AD patients, whereas ADAS-Cog is more sensitive for evaluating moderate AD patients. Although not significant, the Clinical Dementia Rating-Sum of the Boxes had a similar trend to that of the NTB for mild patients. These subgroup results aid in the selection of appropriate patient populations for future studies (Salloway et al., 2011.)

The use of biomarkers as primary endpoints is an area that is presently considered a vital component of drug trials for AD by physicians and is under consideration by FDA. Both imaging and CSF biomarkers were incorporated into the trial design (Salloway et al., 2011). Volumetric MRI was assessed from baseline to week 78 with ventricular volume the primary readout measure, with the inclusion of whole brain volume, hippocampal volume, and cortical ribbon thickness as exploratory measures. The well-characterized CSF biomarkers Aβx-40, Aβx-42, total tau, and phospho-tau181 were measured for changes seen between baseline and 24 weeks (steady state) or 78 weeks. *scyllo*-Inositol at 250mg dose showed a significant increase in ventricular volume compared to placebo controls although the magnitude of the change was small (Salloway et al., 2011). This finding is consistent with previous active and passive immunization trials for AD (Fox et al., 2005; Rinne et al., 2010). None of the other imaging exploratory measures were significant. The CSF biomarkers measured at 24 weeks were not significantly different from baseline; however, at 78 weeks, Aβ42 was significantly lower than placebo. These results are consistent with the CSF Aβ42 levels obtained after a 30-day treatment of TgCRND8 mouse model of AD (McLaurin, unpublished data). The efficacy of *scyllo*-inositol was not determined in this phase II trial as the power of the study was decreased due to the removal of the highest two doses. This study further established the safety profile of *scyllo*-inositol (Salloway et al., 2011). Investigation of *scyllo*-inositol as a therapeutic for AD continues as the understanding of AD evolves both pathologically and clinically.

VI. Structure–Function Analysis of *scyllo*-Inositol

Many AD clinical trials have been initiated over the last 10 years, none of which have shown efficacy as a disease modifying treatment. The failure of these compounds may be attributed to many factors beyond the lack of compound efficacy involving poor trial design, such as targeting the wrong patient population, utilizing the wrong outcome measures, or underdeveloped preclinical data thereby overestimating potential effect size. It is becoming clear that in order to design better clinical trials with an improved ability to determine disease modifying potential, one must have a detailed understanding of the preclinical measures both directly and indirectly effected by a specific compound. In light of this, the investigation into the structure–function relationship between *scyllo*-inositol and Aβ42 both *in vitro* and *in vivo* continued during clinical development.

In order to determine the binding properties that are necessary to elicit the antiaggregation activity of *scyllo*-inositol, a series of compounds substituting the hydroxyl groups with alternative functional groups were synthesized (Sun et al., 2008). The derivatives were designed to investigate the role

of both hydrogen bonding and hydrophobic interactions to the Aβ binding motif. Previous studies using inositol stereoisomers demonstrated that the all equatorial positions of the hydroxyl groups results in the most effective aggregation inhibitor and therefore was maintained in the new compounds (McLaurin et al., 2000). However, the role of each hydroxyl group as well as the hydrophobic face of the ring structure may play varying roles in efficient binding. The chemical equivalency of the *scyllo*-inositol structure allows investigation of the entire surface using substitutions at two opposing sites on the ring. Derivatives of *scyllo*-inositol were synthesized and each derivative was incubated with Aβ42 to examine inhibition of aggregation (Sun et al., 2008). Removal of one or two hydroxyl groups forming 1-deoxy-*scyllo*-inositol or 1,4-dideoxy-*scyllo*-inositol, respectively, resulted in the formation of fibers comparable to that of Aβ42 aggregation alone (Sun et al., 2008). This indicates that all hydroxyl groups are required to inhibit Aβ42 aggregation. To determine the extent hydrogen bonding contributes to this inhibition, fluorine and chlorine substitutes were synthesized. A conservative substitution with fluorine was tested because fluorine is similar in size and polarity to oxygen and it is able to act as a weak hydrogen bond acceptor, while chlorine cannot. Aβ42 incubation with 1-deoxy-1-fluoro-*scyllo*-inositol showed small amorphous aggregates, similar to the inhibitory effect of *scyllo*-inositol. However, 1,4-dideoxy-1,4-difluoro-*scyllo*-inositol was less effective (Sun et al., 2008). Single chlorine substitution showed a weaker inhibitory effect than single fluorine substitution, while the double chlorine substitution resulted in enhanced fibrillogenesis (Sun et al., 2008). To test the role of hydrophobicity, methyl groups were added, which increases the hydrophobic properties of *scyllo*-inositol and if important may enhance inhibition. 1-O-methyl-*scyllo*-inositol has an anti-aggregation effect by stabilizing protofibrillar Aβ42; whereas, two methyl substituted hydroxyl groups, 1,4-di-O-methyl-*scyllo*-inositol, showed fewer and shorter fibers than Aβ42 alone. These studies confirm the necessity for all six hydroxyl groups positioned equatorially around the inositol ring for optimal stabilization of small nontoxic Aβ42 oligomers.

The anti-Aβ-aggregation effects of 1-deoxy-1-fluoro-*scyllo*-inositol and 1,4-di-O-methyl-*scyllo*-inositol were further investigated *in vivo* because it was postulated that they may represent novel positron emission tomography (PET) imaging agents of soluble Aβ.

A. 1-deoxy-1-fluoro-*scyllo*-Inositol

1-deoxy-1-fluoro-*scyllo*-inositol is an analogue of *scyllo*-inositol with a conservative substitution of fluorine for a hydroxyl group at the C1 position of the inositol ring. In general terms, a fluorine substitution not only enhances adsorption, distribution, and metabolic stability, it can also improve protein–ligand binding (Muller et al., 2007). Incubation of

1-deoxy-1-fluoro-*scyllo*-inositol with Aβ42 resulted in small amorphous aggregates that bind the β-structure specific dye thioflavin T, similar to the parent compound *scyllo*-inositol (Hawkes et al., 2012; Sun et al., 2008). In order to determine whether the fluorine substitution would affect CNS bioavailability, 1-deoxy-1-fluoro-*scyllo*-inositol was assessed in an SMIT-1/2 transporter assay, which showed active transport suggesting oral administration would be efficient. When administered to the TgCRND8 mouse model of AD, improvement in spatial memory deficits was observed. Prophylactically, 1-deoxy-1-fluoro-*scyllo*-inositol showed a dose-dependent improvement in spatial memory with the highest dose eliciting spatial memory equivalent to that of the nontransgenic littermates (Hawkes et al., 2012). To correlate improved spatial memory with pathological markers of AD, cerebral Aβ load was analyzed. Total Aβ40 and Aβ42 levels did not change with 1-deoxy-1-fluoro-*scyllo*-inositol treatment, yet Aβ plaque load was decreased (Hawkes et al., 2012). Along with this observation, histological investigation demonstrated that microglial cells, distributed throughout the hippocampus and cortex, have processes that contain intracellular Aβ. The highest dose of 1-deoxy-1-fluoro-*scyllo*-inositol treated TgCRND8 mice showed a significant increase in Aβ-positive microglia in the hippocampus compared to untreated TgCRND8 mice (Hawkes et al., 2012). These brain-resident microglia were not associated with Aβ plaques. These results demonstrate that Aβ bound to 1-deoxy-1-fluoro-*scyllo*-inositol was taken up by microglial cells within the brain and targeted for degradation. To determine whether intra-brain degradation is a mechanism for *scyllo*-inositol effects, a similar histological investigation demonstrated a dose-dependent increase in microglial-associated Aβ after *scyllo*-inositol treatment (McLaurin, unpublished results). These findings are consistent with the decrease in CSF Aβ after *scyllo*-inositol treatment in this mouse model as well as the human Phase II clinical trial and demonstrate that *scyllo*-inositol bound Aβ is degraded within the CNS. Furthermore, the beneficial effects of 1-deoxy-1-fluoro-*scyllo*-inositol further demonstrate the potential for translation to a PET imaging agent for AD.

B. 1,4-di-O-methyl-*scyllo*-Inositol

Similar to 1-deoxy-1-fluoro-*scyllo*-inositol, *in vivo* studies with 1,4-di-O-methyl-*scyllo*-inositol yielded favorable results. *In vitro* studies showed that 1,4-di-O-methyl-*scyllo*-inositol prevented Aβ42 fibrillization by stabilizing Aβ42 protofibrils (Hawkes et al., 2010; Shaw et al., 2011). Prophylactic treatment with 1,4-di-O-methyl-*scyllo*-inositol to TgCRND8 mice also reduced escape latency in the Morris water maze test in a dose-dependent manner, indicating a rescue of spatial memory. However, treatment did not improve spatial memory to that of the nontransgenic littermates (Hawkes et al., 2010). Analysis of Aβ levels in the

brain revealed a decrease in insoluble Aβ42 levels with a concomitant increase in soluble levels. No change in Aβ40 levels was observed, while plaque load was decreased by 30%. Taken together, the decrease in insoluble Aβ and increase in soluble Aβ could be explained by the significant increase in monomeric Aβ after 1,4-di-O-methyl-*scyllo*-inositol treatment (Hawkes et al., 2010). The changes in Aβ42 but not Aβ40 suggested that this compound would not have the specificity necessary for Aβ PET imaging in AD.

C. Positron Emission Tomography Radiopharmaceuticals Based on *scyllo*-Inositol

A number of groups simultaneously have been developing PET radiopharmaceuticals based on *scyllo*-inositol (Elmaleh et al., 2010; Shoup et al., 2009; Vasdev et al., 2009). The first hurdle was to develop a synthetic scheme that renders a high radiochemical yield with a minimum of steps and maintenance of the stereospecificity. Two distinct synthetic schemes have been published that produced [^{18}F]-1-deoxy-1-fluoro-*scyllo*-inositol (Vasdev et al., 2009) and one scheme for production of 2-[^{18}F]fluoro-2-deoxy-*scyllo*-inositol (Pal et al., 2009). The highest radiochemical yield being synthesized from a very stable multifunctional precursor, 1,6;3,4-bis-[*O*-(2,3-dimethoxybutane-2,3-diyl)]-2-*O*-trifluoromethanesulphonyl-5-*O*-benzoyl-*myo*-inositol, in 80min (Vasdev et al., 2009). No matter which synthetic scheme was utilized, small animal imaging studies demonstrated very low brain penetration and high accumulation in the kidneys. Acetylation of the tracer increased brain penetrance; however, it was still below the standard for successful translation of CNS radiotracers to humans (Shoup et al., 2009). An alternate approach synthesized a series of *scyllo*-inositol derivatives attached to 2-ethyl-8-methyl-2,8-diazospiro-4,5-decan-1,3-dione to improve bioavailability (Elmaleh et al., 2010). The radiofluorination yields were high and brain uptake was greater than those reported for the PIB compound in rodents. These compounds are undergoing further investigation to determine their potential translation to AD patients.

D. Development of Novel Compounds Based on *scyllo*-Inositol

To further determine an optimal structural backbone based on *scyllo*-inositol for translation into more effective aggregation inhibitors or PET radiopharmaceuticals, establishment of a screening process was required (Shaw et al., 2011). The criterion for the development of a novel compound was stabilization of low molecular weight nontoxic oligomeric Aβ42 species, as was determined for the parent compound *scyllo*-inositol. The work plan was developed to address the effect of *scyllo*-inositol-based compounds on both structure and toxicity of Aβ. Stabilization of oligomeric Aβ species

was determined using an oligomeric specific ELISA assay, followed by structural determination using atomic force microscopy to rule out presence of amyloid fibers. It is well known that Aβ oligomers are toxic, therefore compounds that favor the stabilization of oligomers may enhance toxicity requiring toxicity assay inclusion.

Using this compound screening protocol, *scyllo*-inositol-based compounds with various substitutions were tested to optimize a backbone structure with maximal Aβ anti-aggregation/binding properties. The compounds were carefully chosen to maintain the polar periphery of the inositol ring, while allowing the exploration of potential hydrophobic binding sites. *scyllo*-Inositol was linked through either aldoxime, hydroxamate, carbamate, or amide to generate novel *scyllo*-inositol derivatives. Of the structures tested, oxime is the only linkage that positioned the phenyl substitution coplanar to the *scyllo*-inositol ring. This co-planar aromatic conformation is analogous to the aromatic structure of polyphenols, which are inhibitors of fiber formation (Bastianetto et al., 2008). Application of the polyphenol-Aβ structure–function relationship to the phenyl ring with oxime linkage to *scyllo*-inositol did not yield favorable oligomerization profile or improve inhibition of fiber formation compared to *scyllo*-inositol; thus distinguishing these flat aromatic compounds from previously reported polyphenols (Bastianetto et al., 2008). Electrospray ionization Orbitrap high-resolution mass spectrometry revealed strong binding between of the phenyl- and napthyl-oxime derivatives to Aβ42 and less stable binding between the azide derivative and Aβ42 (Shaw et al., 2011). These studies demonstrate a backbone structure that now can be utilized to develop more efficient aggregation inhibitors as well as radiopharmaceuticals for PET imaging.

VII. Inositol for the Treatment of Other Disorders

The use of inositol stereoisomers as treatment paradigms for disease has been extensively investigated. *myo*-Inositol, *epi*-inositol, and D-*chiro*-inositol have been examined for their potential therapeutic benefit to treat a variety of conditions ranging from depression to neural tube defects (reviewed in Fenili et al., 2007, 2010). However, the therapeutic properties of *scyllo*-inositol had not been investigated until 2006 (McLaurin et al., 2006). Since then other groups have corroborated the effectiveness of *scyllo*-inositol as a potential AD therapeutic. Interestingly *scyllo*-inositol has recently been proposed for potential therapeutic effectiveness in other conditions based on AD clinical trial data, involvement of Aβ in other disorders, and preclinical model studies.

The phase II clinical trial for AD demonstrated a positive clinical laboratory finding that has the potential to be translated to a number of diseases

associated with hyperuricemia (Cedarbaum, 2010). The clinical laboratory serum analyses demonstrated a *scyllo*-inositol-induced dose-dependent decrease in uric acid (Salloway et al., 2011). Hyperuricemia has been shown to be associated with, represent a risk factor for, or exacerbate certain diseases such as gout, renal disease, cardiovascular disease, metabolic syndrome, urate lithiasis, atherocleropathy, and hypertension. It was therefore proposed that *scyllo*-inositol may have beneficial effects in these disorders.

Further, the results of the phase II clinical trial, for *scyllo*-inositol treatment of AD, brought attention to the positive role of *scyllo*-inositol in reducing the development of neuropsychiatric symptoms in moderate AD patients (Salloway et al., 2011). Thus, it has been proposed that *scyllo*-inositol may have additional uses in the treatment of psychiatric disorders such as bipolar disease (http://newsroom.elan.com/phoenix.zhtml?c=88326&p=irol-newsArticle&ID=1634478&highlight=). The utility of *scyllo*-inositol in these or related disorders will need to wait further consultation with experts and appropriate proof of concept Phase II clinical trials.

Investigation into the potential utility of *scyllo*-inositol for the treatment of macular degeneration was initiated based on the role of Aβ accumulation during retina degeneration (Cruz, 2010). Macular degeneration is characterized by progressive loss of central vision and is the leading cause of blindness in the aging population. Risk factors associated with AD, ApoE genotype, and high cholesterol diet are also risk factors for macular degeneration (Cruz, 2010). In mouse models of age-related macular degeneration, *scyllo*-inositol prevented retinal defects associated with high cholesterol diet (Cruz, 2010). These preclinical mouse studies demonstrate the potential for *scyllo*-inositol effect in age-related macular degeneration; however, clinical investigations will need to be done to prove a cause-effect for this disorder.

The use of a single compound for the treatment of multiple aggregation prone proteins has been extensively investigated with considerable success in preclinical models. The potential translation of *scyllo*-inositol to other neurodegenerative disorders has also been investigated. Vekrellis and colleagues demonstrated that *scyllo*-inositol could rescue the caspase-dependent non-apoptotic death induced by overexpression of wildtype α-synuclein in a human neuronal cell line (Vekrellis et al., 2009). The potential of *scyllo*-inositol to inhibit other aggregation prone proteins will need further preclinical data in both cellular and animal models.

scyllo-Inositol and *myo*-inositol have also been investigated for effects on pentylenetetrazol-(PTZ) induced seizures in rats (Nozadze et al., 2011). PTZ is a $GABA_A$ antagonist that is used to generate animal models of epilepsy. PTZ induces convulsions similar to petit mal or absence seizures in humans. Substances able to modify the threshold for different phases of the convulsions or decrease duration of the seizure in animal models are considered to be antiepileptic (Dhir, 2012). Both *scyllo*-inositol and *myo*-inositol showed anticonvulsant properties, as they significantly reduced seizure

score, delayed the latent period for seizure onset, and decreased seizure duration (Nozadze et al., 2011). Although there were no significant differences between the *myo*- and *scyllo*-inositol treated groups it was found that *scyllo*-inositol was effective at a much lower dose compared to *myo*-inositol (Nozadze et al., 2011).

The investigation of [^{18}F]-1-deoxy-1-fluoro-*scyllo*-inositol for use in cancer as an alternate to the present standard, [^{18}F]2-fluoro-2-deoxy-D-glucose (FDG), was initiated after it was realized that peripheral tissues express SMIT1/2 (McLarty et al., 2011; Vasdev et al., 2009). Furthermore, follow up studies in breast cancer patients result in a high rate of false-positive readings as areas of inflammation have high FDG uptake and similarly high FDG uptake in the brain confounds use for detection of brain metastases (Cook, 2007). The proof of concept rodent studies utilized three human breast cancer or glioma xenograft models and turpentine-oil-induced inflammation to compare peripheral uptake of [^{18}F]-1-deoxy-1-fluoro-*scyllo*-inositol with FDG. An intracranial graft of a human glioblastoma multiforme, U-87, was successfully visualized by PET with both [^{18}F]-1-deoxy-1-fluoro-*scyllo*-inositol and FDG. The uptake of [^{18}F]-1-deoxy-1-fluoro-*scyllo*-inositol in all breast cancer and glioma xenografts was comparable or lower than FDG; however [^{18}F]-1-deoxy-1-fluoro-*scyllo*-inositol accumulated to a lesser degree in inflammation than FDG suggesting an improvement in the ability to distinguish tumor from inflammatory tissue (McLarty et al., 2011). The brain uptake associated with the intracranial glioma over normal tissue for [^{18}F]-1-deoxy-1-fluoro-*scyllo*-inositol was fivefold greater than that for FDG. Due to the enhanced contrast the glioma was more easily visualized utilizing [^{18}F]-1-deoxy-1-fluoro-*scyllo*-inositol and demonstrates a viable opportunity for imaging brain tumors. These studies are ongoing both at the mechanistic and translational level.

VIII. Conclusion

The combined preclinical and clinical data that have been generated surrounding *scyllo*-inositol treatment of Aβ-related diseases, with the predominant disease Alzheimers, have also generated great interest in this naturally occurring compound. Since the first report in 2000 on Aβ-inositol interactions, many groups have contributed to our understanding of the structure–function relationship both *in vitro* and *in vivo*. The transition to human clinical trials in a population that will most benefit from this treatment is still under investigation, although as presented, the possibilities are extensive. Further understanding of the down-stream mechanisms that are altered after removal of toxic Aβ species from the brain by *scyllo*-inositol are presently underway and may lead to new understanding of disease progression.

Acknowledgments

The authors acknowledge funding support from the Canadian Institutes of Health Research (J.M.: PRG 37857; CPG-95275), Natural Science and Engineering Research Council of Canada (JM: CHRP-365537), Alzheimer's Society of Canada Research Program (KM; Grant 300374), Peterborough KM Hunter Graduate Studentship (KM; 2010-2011), University of Toronto Fellowship (LT; 2011), and Norman Stuart Fellowship (LT; 2011).

Conflict of Interest Statement: KM and LT declare no conflict of interest. JM is named inventor on patents relating to *scyllo*-inositol.

Abbreviations

Acetyl-CoA	acetyl-coenzyme A
Aβ	amyloid beta peptide
ADAS-Cog	Alzheimer's disease assessment scale cognitive subscale
ADCS-ADL	Alzheimer's disease cooperative study-activities of daily living
ApoE	apolipoprotein E
APP	amyloid precursor protein
BBB	blood–brain barrier
BID	bis in die (twice daily)
CDR-SB	clinical dementia rating-sum of boxes
CNS	central nervous system
CSF	cerebral spinal fluid
DEAE	diethylaminoethyl
FAD	familial Alzheimers disease
FDA	Food and Drug Administration
FDG	[^{18}F]2-fluoro-2-deoxy-D-glucose
	N-terminus —Amino terminus
$GABA_A$	gamma-aminobutyric acid receptor A
HMIT	proton/*myo*-inositol transporter
ICV	intracerebroventricular
LTP	long-term potentiation
MRI	magnetic resonance imaging
MRS	magnetic resonance spectroscopy
NAD+	nicotinamide adenine dinucleotide (electron accepting form)
NADP+	nicotinamide adenine dinucleotide phosphate
NGF	nerve growth factor
NPI	neuropsychiatric inventory
NTB	neuropsychological test battery
NT2-N	teratocarcinoma-derived Ntera2/D1 neuron-like cells
PC-12	pheochromocytoma cells 12
PET	positron emission tomography

PIB	Pittsburg compound B
PTZ	pentylenetetrazol
SLC5A3	solute carrier family five, member three
SMIT1	sodium/*myo*-inositol transporter one
SMIT2	sodium/*myo*-inositol transporter two
TEAE	treatment emergent adverse side effects
VSOAC	volume-sensitive organic osmolyte-anion channel

References

Anderson, C., & Wallis, E. S. J. (1948). The catalytic hydrogenation of polyhydric phenols. I. The synthesis of *meso*-inositol, scyllitol and a new isomeric cyclitol. *American Chemical Society*, *70*, 2931–2935.

Angyal, S. J., & Matheson, N. K. (1955). Cyclitols. III. Some tosyl esters of inositols. Synthesis of a new inositol. *Journal of American Chemical Society*, *77*, 4343–4346.

Angyal, S. J., Odier, L., & Tate, M. E. (1995). A simple synthesis of *cis*-inositol. *Carbohydrate Research*, *266*, 143–146.

Aytan, N., Carreras, I., Choi, J.-K., Kowall, N. W., Jenkins, B. G., & Dedeoglu, A. (2011). *Effects of scyllo-inositol in a novel transgenic model of Alzheimer's disease*. http://www.sfn.org/am2011/index.aspx?pagename=final_program.

Balandrin, M. F., Klocke, J. A., Wurtele, E. S., & Bollinger, W. H. (1985). Natural plant chemicals: Sources of industrial and medicinal materials. *Science*, *228*, 1154–1160.

Bastianetto, S., Krantic, S., & Quirion, R. (2008). Polyphenols as potential inhibitors of amyloid aggregation and toxicity: Possible significance to Alzheimer's disease. *Mini Reviews in Medicinal Chemistry*, *8*, 429–435.

Berry, G. T., Mallee, J. J., Kwon, H. M., Rim, J. S., Mulla, W. R., Muenke, M., et al. (1995). The human osmoregulatory Na^+/*myo*-lnositol cotransporter gene (SLC5A3): Molecular cloning and localization to chromosome 21. *Genomics*, *25*, 507–513.

Berry, G. T., Wu, S., Buccafusca, R., Ren, J., Gonzales, L. W., Ballard, P. L., et al. (2003). Loss of murine Na^+/*myo*-inositol cotransporter leads to brain *myo*-inositol depletion and central apnea. *Journal of Biological Chemistry*, *278*, 18297–18302.

Bissonnette, P., Coady, M. J., & Lapoi, J. (2004). Expression of the sodium–*myo*-inositol cotransporter SMIT2 at the apical membrane of Madin-Darby canine kidney cells. *Journal of Physiology*, *558*, 759–768.

Bissonnette, P., Lahjouji, K., Coady, M. J., & Lapointe, J. (2008). Effects of hyperosmolarity on the Na^+-*myo*-inositol cotransporter SMIT2 stably transfected in the Madin-Darby canine kidney cell line. *American Journal of Physiology. Cell Physiology*, *295*, 791–799.

Bouveault, L. (1894). De *l'isomérie* optique dans les corps a` chaines ferme´es. *Bulletin de la Societe Chimique de Paris*, *11*, 144–147.

Candy, D. J. (1967). Occurrence and metabolism of *scyllo*-inositol in the locust. *Biochemical Journal*, *103*, 666–671.

Cedarbaum, J. M. (2009). United States Patent Application Publication: Methods of treatment of hyperuricemia and associated disease states. application number 12/560,113, *Elan Pharmaceuticals*. US 2010/0152305 A1www.google.com/patents/.

Chishti, M. A., Yang, D., Janus, C., Phinney, A. L., Horne, P., Pearson, J., et al. (2001). Early-onset amyloid deposition and cognitive deficits in transgenic mice expressing a double mutant form of amyloid precursor protein 695. *Journal of Biological Chemistry*, *276*, 21562–21570.

Choi, J.-K., Carreras, I., Dedeoglu, A., & Jenkins, B. G. (2010). Detection of increased *scyllo*-inositol in brain with magnetic resonance spectroscopy after dietary supplementation in Alzheimers disease mouse models. *Neuropharmacology*, *59*, 353–357.

Chung, S. K., & Kwon, Y. U. (1999). Practical synthesis of all inositol stereoisomers from *myo*-inositol. *Bioorganic & Medicinal Chemistry Letters*, *9*, 2135–2140.

Coady, M. J., Wallendorff, B., Gagnon, D. G., & Lapointe, J. (2002). Identification of a novel Na^+/*myo*-inositol cotransporter. *Journal of Biological Chemistry*, *277*, 35219–35224.

Cook, G. J. (2007). Pitfalls in PET/CT interpretation. *Quarterly Journal of Nuclear Medicine and Molecular Imaging*, *51*, 235–243.

Cruz, A. (2009). *United States Patent Application Publication: Treatment of macular degeneration-related disorders*. Application number 12/576,957www.google.com/patents/US20100093648.

DaSilva, K. A., Brown, M. E., Cousins, J. E., Rappaport, R. V., Aubert, I., Westaway, D., et al. (2009). *scyllo-Inositol (ELND005) ameliorates amyloid pathology in an aggressive mouse model of Alzheimer's disease*. www.abstractsonline.com/Plan/ViewAbstract.aspx?. Key={081F7976-E4CD-4F3D-A0AF-E8387992A658}.

Devanand, D. P., Mikhno, A., Pelton, G. H., Cuasay, K., Pradhaban, G., Dileep Kumar, J. S., et al. (2010). Pittsburgh compound B (11C-PIB) and fluorodeoxyglucose (18 F-FDG) PET in patients with Alzheimer disease, mild cognitive impairment, and healthy controls. *Journal of Geriatric Psychiatry Neurology*, *23*, 185–198.

Di Daniel, E., Mok, M. H. S., Mead, E., Mutinelli, C., Zambello, E., Caberlotto, L. L., et al. (2009). Evaluation of expression and function of the H^+/*myo*-inositol transporter HMIT. *BMC Cell Biology*, *10*, 54.

Dihr, A. (2012). Pentylenetetrazol (PTZ) kindling model of epilepsy. *Currunt Protocol in Neuroscience*, *58*, 9.37.1–9.37.12.

Elan Corporation Press Release. (2011). *Elan Provides an Update on ELND005 (scyllo-inositol)*. November 29, 2011http://newsroom.elan.com/phoenix.zhtml?c=88326&p=irol-newsArticle&ID=1634478&highlight=.

Elmaleh, D., Shoup, T., Fu, H., Johnson, K., Selkoe, D., & Fischman, A. (2010). Synthesis and evaluation of a series of *scyllo*-inositol/2-(fluoroethyl)-8-methyl-2,8-diazaspirol[4,5]decane-1,3-dione combined derivatives as potential amyloid-beta polymerization inhibitors and PET oligomer-Abeta probes. *Journal of Nuclear Medicine*, *51*, 1497.

Feng, Y., Wang, X. P., Yang, S. G., Wang, Y. J., Zhang, X., Du, X. T., et al. (2009). Resveratrol inhibits beta-amyloid oligomeric cytotoxicity but does not prevent oligomer formation. *Neurotoxicology*, *30*, 986–995.

Fenili, D., Brown, M., Rappaport, R., & McLaurin, J. (2007). Properties of *scyllo*-inositol as a therapeutic treatment of AD-like pathology. *Journal of Molecular Medicine (Berliner)*, *85*, 603–611.

Fenili, D., Ma, K., & McLaurin, J. (2010). *scyllo*-Inositol: A potential therapeutic for Alzheimer's disease. In A. Martinez (Ed.), *Emerging Drugs and Targets for Alzheimer's Disease* (1, pp. 94–116)). England: Royal Society of Chemistry.

Fenili, D., Weng, Y.-Q., Aubert, I., Nitz, M., & McLaurin, J. (2011). Sodium/*myo*-Inositol transporters: substrate transport requirments and regional brain expression in the TgCRND8 mouse model of amyloid pathology. *PLoS One*, *6*. e24032.

Ferrão-Gonzales, A. D., Robbs, B. K., Moreau, V. H., Ferreira, A., Juliano, L., Valente, A. P., et al. (2005). Controlling β-amyloid oligomerization by the use of naphthalene sulfonates. *Journal of Biological Chemistry*, *280*, 34747–34754.

Fisher, S. K., Novak, J. E., & Agranoff, B. W. (2002). Inositol and higher inositol phosphates in neural tissues: Homeostasis, metabolism and functional significance. *Journal of Neuroscience*, *82*, 736–754.

Fox, N. C., Black, R. S., Gilman, S., et al. (2005). Effects of Abeta immunization (AN1792) on MRI measures of cerebral volume in Alzheimer disease. *Neurology*, *10*, 1563–1572.

Garzone, P., Koller, M., Pastrak, A., Jhee, S. S., Ereshefsky, L., Moran, S., et al. (2009). Oral amyloid anit-aggregation agent ELND005 is measurable in CSF and brain of healthy adult men. *Alzheimer's and Dementia*, *5*(Suppl), 323.

Goodson, J. A. (1920). Constituents of the leaves of. *Helinus ovatus*. *Journal of Chemical Society, Transactions*, *117*, 140–144.

Hager, K., Hazama, A., Kwon, H. M., Loo, D. D., Handler, J. S., & Wright, E. M. (1995). Kinetics and specificity of the renal Na+/*myo*-inositol cotransporter expressed in Xenopus oocytes. *Journal of Membrane Biology*, *143*, 103–113.

Hann, R. M., & Sando, C. E. (1926). Scyllitol from flowering dogwood (*Cornus florida*). *Journal of Biological Chemistry*, *68*, 399–402.

Hakvoort, A., Haselbach, M., & Galla, H. (1998). Active transport properties of porcine choroid plexus cells in culture. *Brain Research*, *795*, 247–256.

Hawkes, C. A., Deng, L. H., Shaw, J. E., Nitz, M., & McLaurin, J. (2010). Small molecule beta-amyloid inhibitors that stabilize protofibrillar structures in *vitro* improve cognition and pathology in a mouse model of Alzheimer's disease. *European Journal of Neuroscience*, *31*, 203–213.

Hawkes, C. A., Deng, L., Fenili, D., Nitz, M., & McLaurin, J. (2012). In *vivo* uptake of β-amyloid by non-plaque associated microglia. *Current Alzheimer Research*. [BSP/CAR/E-Pub/00096].

Hipps, P. P., Holland, W. H., & Sherman, W. R. (1977). Interconversion of *myo*- and *scyllo*-inositol with simultaneous formation of *neo*-inositol by an NADP+ dependent epimerase from bovine brain. *Biochemical and Biophysical Research Communications*, *77*, 340–346.

Holcomb, L., Gordon, M. N., McGowan, E., Yu, X., Benkovic, S., Jantzen, P., et al. (1998). Accelerated Alzheimer-type phenotype in transgenic mice carrying both mutant amyloid precursor protein and presenilin 1 transgenes. *Nature Medicine*, *4*, 97–100.

Holub, B. J. (1986). Metabolism and function of *myo*-inositol and inositol phospholipids. *Annual Review of Nutrition*, *6*, 563–597.

Inoue, K., Shimada, Y., Minami, H., Morimura, A., Miyai, A., Yamauchi, A., et al. (1996). Cellular localization of Na+/*myo*-inositol co-transporter mRNA in the rat brain. *Neuroreport*, *7*, 1195–1198.

Isaacks, R. E., Bender, A. S., Kim, C. Y., Shi, Y. F., & Norenberg, M. D. (1999). Effect of osmolality and anion channel inhibitors on *myo*-inositol efflux in cultured astrocytes. *Journal of Neuroscience Research*, *57*, 866–871.

Ishibashi, K.-I., Tomiyama, T., Nishitsuji, K., Hara, M., & Mori, H. (2006). Absence of synaptophysin near cortical neurons containing oligomer Aβ in Alzheimer's disease brain. *Journal of Neuroscience Research*, *84*, 632–636.

Janus, C., Pearson, J., McLaurin, J., Mathews, P. M., Jiang, Y., Schmidt, S. D., et al. (2000). A beta peptide immunization reduces behavioural impairment and plaques in a model of Alzheimer's disease. *Nature*, *408*, 979–982.

Kage-Nakadai, E., Uehara, T., & Mitani, S. (2011). H+/*myo*-inositol transporter genes, hmit-1.1 and hmit-1.2, have roles in the osmoprotective response in Caenorhabditis elegans. *Biochemical and Biophysical Research Communications*, *410*, 471–477.

Karran, E., Mercken, M., & De Strooper, B. (2011). The amyloid cascade hypothesis for Alzheimer's disease: An appraisal for the development of therapeutics. *Nature Reviews Drug Discovery*, *10*, 698–712.

Kelly, B. L., Vassar, R., & Ferreira, A. (2005). Beta-amyloid-induced dynamin 1 depletion in hippocampal neurons. A potential mechanism for early cognitive decline in Alzheimer disease. *Journal of Biological Chemistry*, *280*(36), 31746–31753.

Klyubin, I., Walsh, D. M., Lemere, C. A., Cullen, W. K., Shankar, G. M., Betts, V., et al. (2005). Amyloid beta protein immunotherapy neutralizes Abeta oligomers that disrupt synaptic plasticity in *vivo*. *Nature Medicine*, *11*, 556–561.

Kokkoni, N., Stott, K., Amijee, H., Mason, J. M., & Doig, A. J. (2006). N-Methylated peptide inhibitors of beta-amyloid aggregation and toxicity. Optimization of the inhibitor structure. *Biochemistry*, *45*, 9906–9918.

Kokubo, H., Kayed, R., Glabe, C. G., Saido, T. C., Iwata, N., Helms, J. B., et al. (2005). Oligomeric proteins ultrastructurally localize to cell processes, especially to axon terminals with higher density, but not to lipid rafts in Tg2576 mouse brain. *Brain Research*, *1045*, 224–228.

Kowarski, C., & Sarel, S. J. (1973). Total stereoselective synthesis of *myo*-, *allo*-, *neo*-, and *epi*-inositols. *Journal of Organic Chemistry*, *38*, 117–119.

Kwon, H. M., Yamauchi, A., Uchida, S., Preston, A. S., Garcia-Perez, A., Burg, M. B., et al. (1992). Cloning of the cDNa for a Na+/*myo*-inositol cotransporter: A hypertonicity stress protein. *Journal of Biological Chemistry*, *267*, 6297–6301.

Lacor, P. N., Buniel, M. C., Chang, L., Fernandez, S. J., Gong, Y., Viola, K. L., et al. (2004). Synaptic targeting by Alzheimer's-related amyloid beta oligomers. *Journal of Neuroscience*, *24*, 10191–10200.

Larner, J., Jackson, W. T., Graves, D. J., & Stamer, J. R. (1956). Inositol dehydrogenase from aerobacter aerogenes. *Archives of Biochemistry and Biophysics*, *60*, 352–363.

Liang, E., Cedarbaum, J., Abushakra, S., Green, M., Yan, L., & Wagg, J. (2009). Population pharmacokinetic analysis of plasma, cerebrospinal fluid and brain ELND005 in patients with mild to moderate Alzheimer's disease. *Alzheimer's and Dementia*, *5*(Suppl), 465.

Lin, X., Ma, L., Fitzgerald, R. L., & Ostlund, R. E., Jr. (2009). Human sodium/inositol cotransporter 2 (SMIT2) transports inositols but not glucose in L6 cells. *Archives of Biochemistry and Biophysics*, *481*, 197–201.

Loveday, D., Heacock, A. M., & Fisher, S. K. (2003). Activation of muscarinic cholinergic receptors enhances the volume-sensitive efflux of *myo*-inositol from SH-SY5Y neuroblastoma cells. *Journal of Neurochemistry*, *87*, 476–486.

Mandel, M., & Hudlicky, T. J. (1993). General synthesis of inositols by hydrolysis of conduritol epoxides obtained biocatalytically from halogenobenzenes: (+)-D-*chiro*-inositol, *allo*-inositol, *muco*-inositol and *neo*-inositol. *Journal of the Chemical Society. Perkin Transaction*, *1*, 741–743.

Matskevitch, J., Wagner, C. A., Risler, T., Kwon, H. M., Handler, J. S., Waldegger, S., et al. (1998). Effect of extracellular pH on the *myo*-inositol transporter SMIT expressed in *Xenopus* oocytes. *Pflugers Archive*, *436*, 854–857.

McLarty, K., Moran, M. D., Scollard, D. A., Chan, C., Sabha, N., Mukherjee, J., et al. (2011). Comparisons of [18F]-1-deoxy-1-fluoro-*scyllo*-inositol with [18F]-FDG for PET imaging of inflammation, breast and brain cancer xenografts in athymic mice. *Nuclear Medicine Biology*, *38*, 953–959.

McLaurin, J., & Chakrabartty, A. (1996). Membrane disruption by Alzheimer β-amyloid peptides mediated through specific binding to either phospholipids or gangliosides. *Journal of Biological Chemistry*, *271*, 26482–26489.

McLaurin, J., & Chakrabartty, A. (1997). Characterization of the interactions of Alzheimer β-amyloid peptides with phospholipid membranes. *European Journal of Biochemistry*, *245*, 355–363.

McLaurin, J., Franklin, T., Chakrabartty, A., & Fraser, P. E. (1998). Phosphatidylinositol and inositol involvement in Alzheimer amyloid-β fibril growth and arrest. *Journal of Molecular Biology*, *278*, 183–194.

McLaurin, J., Golomb, R., Jurewiczi, A., Anteli, J. P., & Fraser, P. E. (2000). Inositol stereoisomers stabilize an oligomeric aggregate of Alzheimer amyloid β peptide and inhibit Aβ-induced toxicity. *Journal of Biological Chemistry*, *275*, 18495–18502.

McLaurin, J., Kierstead, M. E., Brown, M. E., Hawkes, C. A., Lambermon, M. H., Phinney, A. L., et al. (2006). Cyclohexanehexol inhibitors of Abeta aggregation prevent and reverse Alzheimer phenotype in a mouse model. *Nature Medicine*, *12*, 801–808.

McPhie, R. P., & Campana, S. E. (2009). Reproductive characteristics and population decline of four species of skate (Rajidae) off the eastern coast of Canada. *Journal of Fish Biology*, *75*, 233–246.

McVeigh, K. E., Mallee, J. J., Lucente, A., Barnoski, B. L., Wu, S., & Berry, G. T. (2000). Murine chromosome 16 telomeric region, homologous with human chromosome 21q22, contains the osmoregulatory Na(+)/*myo*-inositol cotransporter (SLC5A3) gene. *Cytogenetics and Cell Genetics*, *88*, 153–158.

Michell, R. H. (2008). Inositol derivatives: Evolution and functions. *Nature Reviews Molecular Cell Biology*, *9*, 151–161.

Müller, H. (1907). Cocositol (cocosite), a constituent of the leaves of "Cocos nucifera" and "cocos plumosa". *Journal of the Chemical Society Transactions*, *91*, 1767–1780.

Müller, H. (1912). Inositol and some of its isomerides. *Journal of the Chemical Society Transaction*, *101*, 2383–2410.

Müller, K., Faeh, C., & Diederich, F. (2007). Fluorine in pharmaceuticals: looking beyond intuition. *Science*, *317*, 1881–1886.

Novak, J. E., Agranoff, B. W., & Fisher, S. K. (2000). Regulation of *myo*-inositol homeostasis in differentiated human NT2-N neurons. *Neurochemical Research*, *25*(5), 561–566.

Nozadze, M., Mikautadze, E., Lepsveridze, E., Mikeladze, E., Kuchiashvili, N., Kiguradze, T., et al. (2011). Anticonvulsant activities of *myo*-inositol and *scyllo*-inositol on pentylenetetrazol induced seizures. *Seizure*, *20*, 173–176.

Oakley, H., Cole, S. L., Logan, S., Maus, E., Shao, P., Craft, J. et al. (2006). Intraneuronal beta-amyloid aggregates, neurodegeneration, and neuron loss in transgenic mice with five familial Alzheimer's disease mutations: Potential factors in amyloid plaque formation. *Journal of Neuroscience*, *26*, 10129–10140.

Oddo, S., Caccamo, A., Kitazawa, M., Tseng, B. P., & LaFerla, F. M. (2003). Amyloid deposition precedes tangle formation in a triple transgenic model of Alzheimer's disease. *Neurobiology of Aging*, *24*, 1063–1070.

Ostlund, R. E., Jr., Seemayer, R., Gupta, S., Kimmel, R., Ostlund, E. L., & Sherman, W. R. (1996). A stereospecific *myo*-inositol/D-*chiro*-inositol transporter in HepG2 liver cells. Identification with D-*chiro*-[3-3H]inositol. *Journal of Biological Chemistry*, *271*, 10073–10078.

Pal, A., Mukhapadhyay, U., Volgin, A., Shavrin, A., Tong, W., Gelovani, J., & Alauddin, M. (2009). Radiosynthesis of 2-[18F]fluoro-2-deoxy-*scyllo*-inositol for PET imaging of phosphadtidylinositol pool in PI3 kinase activity. *Journal of Nuclear Medicine*, *50*, 261.

Park, S., Pegan, S. D., Mesecar, A. D., Jungbauer, L. M., LaDu, M. J., & Liebman, S. W. (2011). Development and validation of a yeast high-throughput screen for inhibitors of Aβ42 oligomerization. *Disease Models & Mechanisms*, *4*, 822–831.

Podeschwa, M., Plettenburg, O., vom Brocke, J., Block, O., Adelt, S., & Altenbach, H.-J. (2003). Stereoselective synthesis of *myo*-, *neo*-, L-*chiro*, D-*chiro*, *allo*-, *scyllo*-, and *epi*-inositol systems via conduritols prepared from p-benzoquinon. *European Journal of Organic Chemistry*, *2003*, 1958–1972.

Posternak, T. (1965). Les Cyclitols. *Hermann*, *97*.

Praveen, T., & Shashidhar, M. S. (2001). Convenient synthesis of 4,6-di-O-benzyl-*myo*-inositol and *myo*-inositol 1,3,5-orthoesters. *Carbohydrate Research*, *330*, 409–411.

Prince, M., Bryce, R., & Ferri, C. (2011). *Alzheimer's Disease International World Alzheimer Report 2011 The benefits of early diagnosis and intervention*. January 25, 2012http://www.alz.co.uk/research/WorldAlzheimerReport2011ExecutiveSummary.pdf.

Quinn, K., Brigham, B., Soriano, F., Connop, B., & Sauer, J. M. (2009). ELD005 (*scyllo*-inositol), the β-amyloid anti-aggregation therapeutic, demonstrates robust brain uptake in rats following oral administration. *Alzheimer's and Dementia*, *5*(Suppl), 437.

Ramaley, R., Fujita, Y., & Freese, E. (1979). Purification and properties of Bacillus subtilis inositol dehydrogenase. *Journal of Biological Chemistry*, *254*, 7684–7690.

Reddy, R. E., Chemburkar, S. R., Spaulding, D. R., Pan, Y., Cao, L., Restituyo, J. A., et al. (2011). (United States patent application: Process for the preparation of *scyllo*-inositol). *United States patent application number*, *20110201060*http://patents.com/us-20110201060.html.

Rinne, J. O., Brooks, D. J., Rossor, M. N., et al. (2010). 11C-PiB PET assessment of change in fibrillar amyloid-beta load in patients with Alzheimer's disease treated with bapineuzumab: a phase 2, double-blind, placebo-controlled, ascending dose study. *Lancet Neurology*, *9*, 363–372.

Roll, P., Massacrier, A., Pereira, S., Robaglia-Schlupp, A., Cau, P., & Szepetowski, P. (2002). New human sodium/glucose cotransporter gene (KST1): Identification, characterization, and mutation analysis in ICCA (infantile convulsions and choreoathetosis) and BFIC (benign familial infantile convulsions) families. *Gene*, *285*, 141–148.

Salloway, S., Sperling, R., Keren, R., Porsteinsson, A. P., van Dyck, C. H., Tariot, P. N., et al. (2011). A phase 2 randomized trial of ELND005, *scyllo*-inositol, in mild to moderate Alzheimer disease. *Neurology*, *77*, 1253–1262.

Sanz, M. L., Villamiel, M., & Martinez-Castro, I. (2004). Inositols and carbohydrates in different fresh fruit juices. *Food Chemistry*, *87*, 325–328.

Sarmah, M. P., & Shashidhar, M. S. (2003). Sulfonate protecting groups. Improved synthesis of *scyllo*-inositol and its orthoformate from *myo*-inositol. *Carbohydrate Research*, *338*, 999–1001.

Seaquist, E. R., & Gruetter, R. (1998). Identification of a high concentration of *scyllo*-inositol in the brain of a healthy human subject using 1H- and 13C-NMR. *Magnetic Resonance in Medicine*, *39*, 313–316.

Shaldubina, A., Buccafusca, R., Johanson, R. A., Agam, G., Belmaker, R. H., Berry, G. T., & Bersuds, Y. (2007). Behavioural phenotyping of sodium-*myo*-inositol cotransporter heterozygous knockout mice with reduced brain inositol. *Genes Brain Behavior*, *6*(3), 253–259.

Shankar, G. M., Bloodgood, B. L., Townsend, M., Walsh, D. M., Selkoe, D. J., & Sabatini, B. L. (2007). Natural oligomers of the Alzheimer amyloid-β protein induce reversible synapse loss by modulating an NMDA-type glutamate receptor-dependent signaling pathway. *Journal of Neuroscience*, *27*(11), 2866–2875.

Shaw, J. E., Chio, J., Dasgupta, S., Lai, A. Y., Mo, G. C.H., F.Pang, F., et al. (2011). Assembly in the presence of *scyllo*-inositol derivatives: Identification of an oxime linkage as important for the development of assembly inhibitors. *ACS Chemical Neuroscience*, 1–42. dx. doi.org/10.1021/cn2000926.

Sherman, W. R., Stewart, M. A., Kurien, M. M., & Goodwin, S. L. (1968). The measurement of *myo*-inositol, *myo*-inosose-2 and *scyllo*-inositol in mammalian tissues. *Biochemica et Biophysica Acta*, *158*, 197–205.

Sherman, W. R., Simpson, P. C., & Goodwin, S. L. (1978). *scyllo*-Inositol and *myo*-inositol levels in tissues of the skate Raja erinacea. *Comparative Biochemistry and Physiology B*, *59*. 201–201.

Shim, Y. S., & Morris, J. C. (2011). Biomarkers predicting Alzheimer's disease in cognitively normal aging. *Journal of Clinical Neurology*, *7*, 60–68.

Shoup, T., Elmaleh, D., Carter, E., Winter, D., Tolman, C., & Fischman, A. (2009). Synthesis and biodistribution of F-18 labeled *scyllo*-inositol derivatives as potential probes for decting amyloid beta oligomers. *Journal of Nuclear Medicine*, *50*, 1935.

Soria, A. C., Sanz, M. L., & Villamiel, M. (2009). Determination of minor carbohydrates in carrot (Daucus carota L.) by GC-MS. *Food Chemistry*, *114*, 758–762.

Spector, R. (1976). The specificity and sulfhydryl sensitivity of the inositol transport system of the central nervous system. *Journal of Neurochemistry*, *27*, 229–236.

Sun, Y., Zhang, G., Hawkes, C. A., Shaw, J. E., McLaurin, J., & Nitz, M. (2008). Synthesis of *scyllo*-inositol derivatives and their effects on amyloid beta peptide aggregation. *Bioorganic & Medicinal Chemistry*, *16*, 7177–7184.

Tagliaferri, F., Wang, S.-N., Berlin, W. K., Outten, R. A., & Shen, T. Y. (1990). Glycosylinositol derivatives. I. Synthesis of 1-substituted *chiro*-inositol derivatives. *Tetrahedron Letters*, *31*, 1105–1108.

Takahashi, H., Kittaka, H., & Ikegami, S. (2001). Novel synthesis of enantiomerically pure natural inositols and their diastereoisomers. *Journal of Organic Chemistry*, *66*, 2705–2716.

Townsend, M., Cleary, J. P., Mehta, T., Hofmeister, J., Lesne, S., O'Hare, E., et al. (2006). Orally available compound prevents deficits in memory caused by the Alzheimer amyloid-beta oligomers. *Annals of Neurology*, *60*, 668–676.

Uldry, M., Ibberson, M., Horisberger, J., Chatton, J., Riederer, B. M., & Thorens, B. (2001). Identification of a mammalian H^+-*myo*-inositol symporter expressed predominantly in the brain. *EMBO Journal*, *20*, 4467–4477.

Uldry, M., Steiner, P., Zurich, M., Béguin, P., Hirling, H., Dolci, W., & Thorens, B. (2004). Regulated exocytosis of an H^+/*myo*-inositol symporter at synapses and growth cones. *EMBO Journal*, *23*, 531–540.

Vasdev, N., Chio, J., van Oosten, E. M., Nitz, M., McLaurin, J., Vines, D. C., et al. (2009). Synthesis and preliminary biological evaluations of [18F]-1-deoxy-1-fluoro-*scyllo*-inositol. *Chemical Communications (Cambridge)*, *37*, 5527–5529.

Vekrellis, K., Xilouri, M., Emmanouilidou, E., & Stefanis, L. (2009). Inducible over-expression of wild type α-synuclein in human neuronal cells leads to caspase-dependent non-apoptotic death. *Journal of Neurochemistry*, *109*, 1348–1362.

Walsh, D. M., Klyubin, I., Fadeeva, J. V., Cullen, W. K., Anwyl, R., Wolfe, M. S., et al. (2002). Naturally secreted oligomers of amyloid beta protein potently inhibit hippocampal long-term potentiation *in vivo*. *Nature*, *416*, 535–539.

Watanabe, Y., Mitani, M., & Ozaki, S. (1987). Synthesis of optically active inositol derivatives starting from D-glucurono-6,3-lactone. *Chemistry Letters*, 123–126.

Watanabe, T., Shiino, A., & Akiguchi, I. (2010). Absolute quantification in proton magnetic resonance spectroscopy is useful to differentiate amnesic mild cognitive impairment from Alzheimer's disease and healthy aging. *Dementia and Geriatric Cognitive Disorders*, *30*, 71–77.

Williams, L. J., Cicia, A. M., Pellegrin, G. B., Smith, K. M., & Sulikowski, J. A. (2011). The reproductive cycle of the roundel skate *Raja texana*. *Journal of Fish Biology*, *79*, 298–305.

Yamaguchi, M., Kita, Y., Mori, T., Kanbe, K., Tomoda, A., Takahashi, A., et al. (2004). *United States Patent: Method for producing scyllo-inositol. Hokko Chemicals*. Patent number US7745671: http://www.freepatentsonline.com/7745671.html.

Yamaoka, M., Osawa, S., Morinaga, T., Takenaka, S., & Yoshida, K. (2011). A cell factory of Bacillus subtilis engineered for the simple bioconversion of *myo*-inositol to *scyllo*-inositol, a potential therapeutic agent for Alzheimer's disease. *Microbial Cell Factories*, *10*, 69.

Yap, I. K., Brown, I. J., Chan, Q., Wijeyesekera, A., Garcia-Perez, I., Bictash, M., et al. (2010). Metabolome-wide association study identifies multiple biomarkers that discriminate north and south Chinese populations at differing risks of cardiovascular disease: INTERMAP study. *Journal of Proteome Research*, *9*(12), 6647–6654.

Yoshida, K., Yamaguchi, M., Morinaga, T., Ikeuchi, M., Kinehara, M., & Ashida, H. (2006). Genetic modification of Bacillus subtilis for production of D-*chiro*-inositol, an investigational drug candidate for treatment of type 2 diabetes and polycystic ovary syndrome. *Applied and Environmental Microbiology*, *72*, 1310–1315.

Yoshida, K., Yamaguchi, M., Morinaga, T., Kinehara, M., Ikeuchi, M., Ashida, H., et al. (2008). *myo*-Inositol catabolism in *Bacillus subtilis*. *Journal Biological Chemistry*, *283*, 10415–10424.

Zhao, F., & Keating, A. F. (2007). Functional properties and genomics of glucose transporters. *Current Genomics*, *8*, 113–128.

Zhao, W., Toolan, D., Hepler, R. W., Wolfe, A. L., Yu, Y., Price, E., et al. (2011). High throughput monitoring of amyloid-β42 assembly into soluble oligomers achieved by sensitve confomation state-dependent immunoassays. *Journal of Alzheimer's Disease*, *25*, 655–669.